Optical properties of hybrid organic-inorganic materials and their applications – Part I: Luminescence and Photochromism

Stephane Parola, Beatriz Julián-López, Luís D. Carlos, Clément Sanchez

Prof. S. Parola
Laboratoire de Chimie ENS Lyon, Université de Lyon, Ecole Normale Supérieure de Lyon, Université Lyon 1, CNRS UMR 5182, 46 allée d'Italie, 69364 Lyon, France.

Dr. B. Julián-López
Department of Inorganic and Organic Chemistry - INAM, University Jaume I, Castellón de La Plana 12071, Spain.

Prof. L. D. Carlos
Univ Aveiro, Dept Phys, P-3810193 Aveiro, Portugal
Univ Aveiro, CICECO – Aveiro Institute of Materials, P-3810193 Aveiro, Portugal

Prof. C. Sanchez
Collège de France, UMR 7574, Laboratoire Chimie de la Matière Condensée Paris, F-75005 Paris, France.

Keywords: hybrid materials, optics, photonics, plasmonics, luminescence

(Abstract: Research on hybrids inorganic-organic materials has experienced an explosive growth since the 1980s, with the expansion of soft inorganic chemistry based processes. Indeed, mild synthetic conditions, low processing temperatures provided by "chimie douce" and the versatility of the colloidal state allow for the mixing of the organic and inorganic components at the nanometer scale in virtually any ratio to produce the so called hybrid materials. Today a high degree of control over both composition and nanostructure of these hybrids can be achieved allowing tunable structure-property relationships. This, in turn, makes it possible to tailor and fine-tune many properties (mechanical, optical, electronic, thermal, chemical…) in very broad ranges, and to design specific multifunctional systems for applications. In particular, the field of "Hybrids-Optics" has been very productive not only scientifically but also in terms of applications. Indeed, numerous optical devices based on hybrids are already in, or very close, to the market. This review describes most of the recent advances performed in this field. Emphasis will be given to luminescent, photochromic, NLO and plasmonic properties. As an outlook we show that the controlled coupling between plasmonics and luminescence is opening a land of opportunities in the field of "Hybrids-Optics".)

1. Introduction

The field of hybrid organic-inorganic materials has been growing intensively during the past 20 years and is certainly nowadays one of the major fields of research and unambiguously one of the most exciting. The idea to combine organic and inorganic systems appears now has evidence, but considering the complexity to design association of materials that exhibit very low compatibility for each other's, it has led the chemists and physicist to imagine numerous architectures more or less easy to achieve experimentally. The rising of new characterization techniques and knowledge at the nanometer scale and even the molecular scale has been a driving force towards imagination of hybrid architectures in many major fields such as

sensors, electronics, optics, lightning, medicine, catalysis, energy storage, energy conversion. Moreover, the need for always better materials for complex devices with improved properties and multifunctional responses is a perpetual demand which often can be fulfilled by the use of hybrid materials. In particular, regarding the broad field of optical materials, ranging from lightning to energy, bioimaging, screens design, optoelectronics and many others, the design of hybrid materials has been particularly productive (**Figure 1**). One reason is that combining unique optical responses of organic or organometallic molecular species with either mechanical properties or optical properties of inorganic counterparts provides a unique way to elaborate highly innovating optical systems at the macro or the nanoscale. Considering the usually high sensitivity of optical responses to the environment, the interfaces between the organics and inorganics is a crucial parameter in most systems. Of course, large number of books and reviews were previously published in the different fields related to optics, both by chemists, physicists and biologists showing the large community concerned by this topic. This article aims to review the latest reported hybrid optical materials, with strong focus on the 10 last years, and trying to make an overview of the relationship between the structures and the measured properties, as well as the way to control the interfaces in the hybrids. Regarding the number of work in the field, this report cannot be exhaustive, but can give an insight in the actual state of the art in the field of hybrid materials devoted to optics and in particular the relationship between the different types of structure, the organic-inorganic interfaces and the final properties of the systems.

Figure 1. Hybrid materials and optical properties, from ancient time and art design to highly innovative functional devices.

2. Light-emitting hybrid materials

2.1 Introduction to luminescence

Luminescence is a general term that describes any non-thermal processes in which energy is emitted in the ultraviolet, visible or infrared spectral regions from an electronically excited species. Generally, the emission occurs at a higher wavelength from that at which light is

absorbed (a process termed as downshifting). The term broadly includes the commonly used categories of fluorescence and phosphorescence, depending upon the electronic configuration of the excited state and the emission pathway.[1, 2] The distinction between the various types of luminescence is usually made according to the mode of excitation. For instance, Bioluminescence is related with light emission from lived animals and plants, Cathodoluminescence results from excitation by electron beams, Chemiluminescence is the emission occurring during a chemical reaction, Radioluminescence is produced by ionizing radiation (α, β, γ, and X-rays), Triboluminescence is ascribed to rubbing, mechanical action, and fracture, Electroluminescence is the conversion of electrical energy into light, and Photoluminescence results from excitation by photons.

In a first order absorption process, when the photon energy of the incident radiation is lower than the energy difference between two electronic states, the photons are not absorbed and the material is transparent to such radiation energy. For higher photons energy, absorption occurs (typically in 10^{-15} s) and the valence electrons will make a transition between two electronic energy levels. The excess of energy will be dissipated through vibrational processes that occur throughout the near infrared (NIR) spectral region. If this transition does not involve spin inversion, the excited state is also a singlet (S), *i.e.*, has the same state multiplicity as the ground level (S_0). However, if there is spin inversion, the two electrons have the same spin, S=1 and 2S+1=3, and the excited state is called a triplet (T). Then, the excited atoms may return to the original level through radiative (fluorescence or phosphorescence) and non-radiative transitions (internal conversion) (**Figure 2**). It should be noted that an absorption involving a triplet state is forbidden by the spin selection rule: allowed transitions must involve the promotion of electrons without a change in their spin (ΔS=0). The relaxation of the spin selection rule can occur though strong spin-orbit coupling, which is, for instance, what happens in the case of Ln^{3+} ions.

Examples of non-radiative processes

- Internal conversion; an electron close to a ground state vibrational energy level, relaxes to the ground state via transitions between vibrational energy levels giving off the excess energy to other molecules as heat (vibrational energy). The time scale of the internal conversation and vibrational relaxation processes is 10^{-14}–10^{-11} s.
- Intersystem crossing; the electron transition in an upper S_1 excited state to a lower energy level, such as T_1.
- Delayed fluorescence; after a fast intersystem crossing to T_1 and a thermally popped back into S_1. The lifetime of S_1 increases and, in the limit, would be nearly equal to the lifetime of T_1.[3] Delayed fluorescence can also occurs when two excited states interact and annihilate forming an emitting state, *e.g.* in triplet-triplet annihilation.[4, 5] Triplet–triplet annihilation is an encouraging up-conversion approach due to its low excitation power density (solar radiation is enough), high quantum yield, tunable excitation/emission wavelength and strong absorption.[6]

Examples of radiative processes

- Fluorescence; emission of a photon from S_1 to the vibrational states of S_0 occurring in a time scale of 10^{-9} to 10^{-7} s.
- Phosphorescence; emission of a photon from T_1 to the vibrational sates of S_0. This process is much slower than fluorescence (10^{-3}–10^{2} s) because it involves two states of distinct multiplicity. For very long luminescence time decays (minutes and even hours), the emission is called persistent luminescence or afterglow.

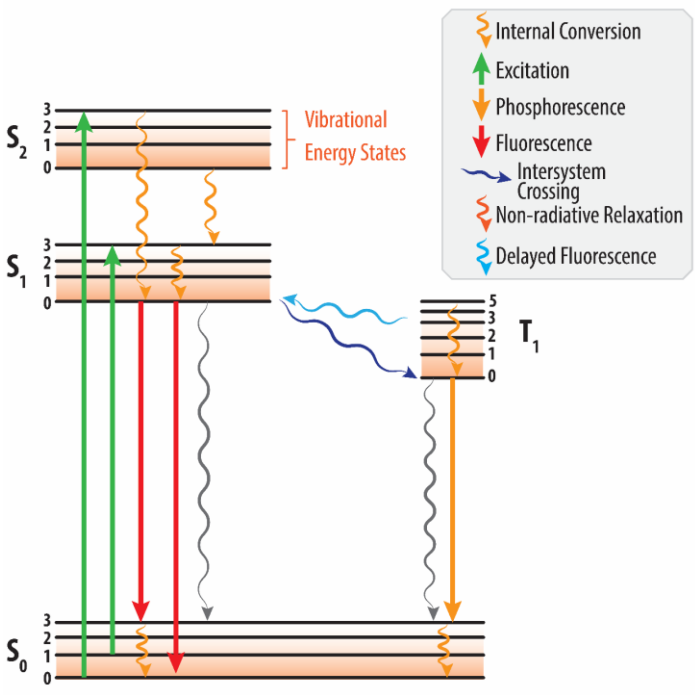

Figure 2. Jablonski diagram summarizing the typical radiative and non-radiative transitions within an electronically excited specie.

Due to the non-radiative transitions, fluorescence and phosphorescence will occur at lower energy (longer wavelengths) than that of the absorbed photons. The energetic difference between the maximum of the emission and absorption spectra ascribed to the same electronic transition is known as Stokes–shift.[7]

Electroluminescence results from the radiative recombination of electrons and holes injected into an inorganic, organic or organic-inorganic hybrid semiconductor material. Electroluminescence devices include light emitting diodes (LEDs), which produce light when a current is applied to a doped p-n junction of a semiconductor, and matrix-addressed displays.[7] In the past decades, LEDs and organic light-emitting diodes (OLEDs) induced a deep revolution in the lighting industry. The first examples of the use of hybrid materials in lighting (more specifically in solid-state lighting, SSL) appeared in 2001 with layered crystalline organic-inorganic perovskites.[8] Although the interest on these hybrid perovskites as single-phase white light emitters continue,[9, 10] the wide range of materials with potential application in SSL would include dye-bridged,[11-17] dye-doped[18] and quantum dots-doped[19] siloxane-based organic-inorganic hybrids, and metal organic frameworks.[20] Despite the interest of organic-inorganic hybrid perovskites in lighting, the most exciting application of these materials is in solar cells. Perovskite solar cells have shown remarkable progress in the last decade, with rapid increases in conversion efficiency, from 3.8% in 2009[21] to 20% in 2015,[22] demonstrating the potential competitiveness to traditional commercial solar cells and offering the prospective for an earth-abundant and low-energy-production solution to large-scale manufacturing of photovoltaic modules.[23]

The potential of light-emitting hybrid materials relies on the possibility of fully exploiting the synergy between the optical features of the emitting centers and the intrinsic characteristics of the sol-gel derived hosts. Hybrid materials present several advantages for photonic and optical applications, such as: i) versatile shaping and patterning, depending on the foreseen

application; ii) optimization of composition and processing conditions, yielding excellent optical quality, high transmission, low processing temperature (< 200 °C), and easy control of the refractive index by changing the relative proportion of the different precursors; and iii) photosensitivity, mechanical integrity, corrosion protection, and suitable adhesion properties.[24-30] In general, the embedding of organic dyes, quantum dots (QDs), and trivalent lanthanide (Ln^{3+}) complexes into hybrid hosts, with the corresponding formation of covalent (Class II) or non-covalent (Class I) [31] host-guest interactions, improves the thermal stability, the mechanical resistance, and the aging and environmental stability of the guest emitting centers, relatively to what is observed for isolated centers.[32, 33] Moreover, the dispersion of these centers within the hybrid framework allows their incorporation in larger amounts, isolated from each other and protected by the hybrid host, improving the emission quantum yield and preventing the emission degradation.[34-38] An illustrative example is the control of the molecular aggregation of chromophores in the solid state, namely the formation of fluorescent J-aggregates instead of non-fluorescent H-aggregates, using fragments of hydrolysable triethoxysilane (TEOS).[12]

In this section, we cover recent developments of luminescent and electroluminescent hybrid materials, with particular emphasis to specific applications, such as LEDs, random and feedback lasers, luminescent solar concentrators (LSCs), and luminescent thermometers. Examples will address organic-inorganic hybrids (essentially siloxane-based ones) embedding organic dyes, with the formation of covalent (dye-bridged hybrids) or non-covalent (dye-doped hybrids) dye-matrix interactions, QDs, inorganic nanoparticles and Ln^{3+} complexes. Hybrids with photochromic features will be discussed in Sec. 3, whereas hybrids for phosphors[39] and for luminescent coatings (based on organic dyes,[40] fluorine polymers,[41] cooper iodide clusters[42] and on Ln^{3+} ions[43-45]) were not reviewed in detail, being only addressed in the context of LEDs and LSCs, respectively. General and comprehensive reviews on luminescent organic-inorganic hybrid materials embedding organic dyes and Ln^{3+} ions were published by Carlos,[25, 28] Sanchez,[27, 46-48] Escribano,[49] Binnemans,[50] Zhang,[51] and Ribeiro.[52] Concerning electroluminescence, there is only one recent review addressing the application of dye-doped hybrids on LEDs.[53] In view of the current trends of the subject, and balancing the literature published since these reviews, we decide to not discuss the applications of luminescent hybrid materials in integrated optics and optical telecommunications, in biomedicine, and in solar cells. While in integrated optics and optical telecommunications the review by Ferreira *et al.*[26] is relatively updated, in solar cells and in biomedicine the amount of work published in the past 5 years justify independent review publications. In fact, perovskite solar cells largely dominate the current research trend of hybrid materials in photovoltaics, while in biomedicine ligand-decorated QDs and Ln^{3+}-based inorganic NPs, Ln^{3+} chelates embedded within inorganic matrices and more complex core-shell and core-corona hybrid architectures have been designed as biosensing platforms for *in vivo* imaging, diagnostics, targeting and therapy. The subject underwent an enormous expansion during the last decade that can be tracked, for instance, in the recent reviews of Prasad *et al.*,[54, 55] Prodi *et al.*,[56] and Bünzli.[57]

2.2 White light emission and LEDs

The interest in organic-inorganic hybrids for LEDs has grown considerably during the last three decades since the seminal work of Tang and VanSlyke on dye-based OLEDs operating at low driving voltages[58] and the first reports demonstrated the possibility of applying these materials in solid-state lasers.[59-61] The first examples of white LEDs (WLEDs) based in organic-inorganic hybrids date back to the final of last century comprising dye-modified silanes incorporating hole- or electron-transporting units and light-emitting species in the orange[62] and green[11] spectral regions. Later on, more efficient WLEDs were reported

involving silsesquioxane hybrid matrices, as, for example, that based on the phenylenevinylenediimide precursor, luminance value of 10 $cd \cdot m^{-2}$ for voltages lower than 30 V,[12] and that based on polyhedral oligomeric silsesquioxanes bearing in the structure a dye molecule from the cyanine family, threshold operating voltage of 4 V.[63] An intriguing example is the fabrication of a WLEDs by coating a commercial UV LED (390 nm) with a periodic mesoporous organosilica (PMO) film doped with Rhodamine 6G (Rh6G) and synthesized by surfactant-templated sol-gel polycondensation using a 1,3,6,8-tetraphenylpyrene (TPPy)-containing organosilane precursor.[13] The blue emission of the films, emission quantum yield of 0.70, overlaps the absorption spectra of the dye and thus efficient energy transfer occurred and the white-light is achieved by combining the blue emission of the host with the yellow light of the guest. UV pumped WLEDs have huge potential because they are easy to manufacture, the white light emission is only due to the down-converting phosphors, they exhibit a low colour point variation as a function of the forward-bias currents, and they have superior temperature stability. Moreover, as the human eyes are insensitive to UV radiation, the white colour is independent of the pumping LED and of the thickness of the phosphor layer.

Poly(2-hydroxyethyl methacylate-silica hybrids doped with organoboron dyes emitting in the blue, green and red spectral regions[16] and dye-bridged epoxy functional oligosiloxanes emitting in the green and red spectral regions with absolute emission quantum yields of 0.85 and 0.41, respectively,[17] were used to produce efficient multi-color light-emitting hybrids. In this latter example, WLEDs were produced using a commercial blue LED as excitation source and by controlling the dyes concentration and the ratio between the red and green emitting species, (**Figure 3**). The best device has a CCT of 4810 K, a CRI of 85 and a luminous efficacy of 23.7 $lm \cdot W^{-1}$, being thermally stable at 120°C for 1200 h.[17]

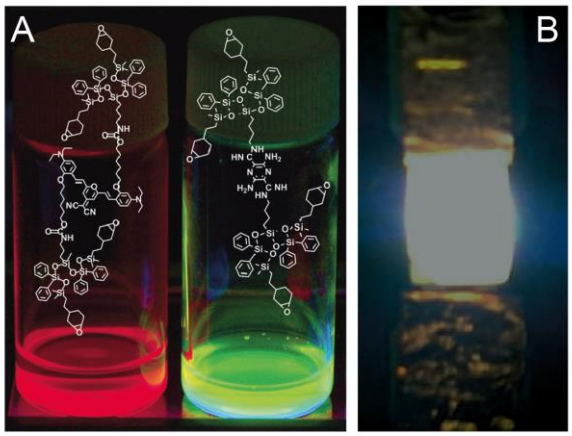

Figure 3. Photographs of A) red and green dye-bridged oligosiloxanes under UV excitation at 365 nm and B) dye-bridged nanohybrid-based white LED, CIE color coordinates of (0.348, 0.334), fabricated encapsulating a blue LED (445 nm) with a blend of red and green dyes. Taken with permission from reference [17]. Copyright (2011) Wiley-VCH.

Other example comprises dye molecules containing trialkoxysilyl terminal groups embedded into silica nanoparticles emitting in the red and yellowish-green spectral regions.[15] In this case, a WLED was fabricated by combining such fluorescent organosilica nanoparticles with a commercial blue InGaN LED. The resulting three-color RGB LED exhibited a CRI of 86.7, a CCT of 5452.6 K and CIE (x,y) coordinates of (0.3334,0.3360).[15]

The possible use of organically doped layered phyllosilicate clays was introduced in the late 90's.[64, 65] Although not fabricated as WLEDs, white light-emitting soft hybrids was reported

based on the supramolecular co-assembly of organoclays and ionic chromophores.[66-68] Layered magnesium phyllo(organo)silicate with aminopropyl pendants (AC in **Figure 4A**) was used as the inorganic counterpart, while coronene tetra-carboxylate (CS), sulforhodamine G (SRG), and tetraphenylethylene derivatives (TPTS) were employed as donor-acceptor organic chromophores (Figure 4A). White light emission was attained via partial excitation energy transfer from the AC-CS hybrid to the co-assembled acceptor SRG dye molecules[66, 67] (Figure 4B) or by in situ photogeneration of a blue component modifying the clay hybrid containing green (TPTS) and red (SRG) emitting components (Figure 4C).[68] The solution processability, high transmittance, color tunability, and the environmentally benign solvent medium of these "softhybrids" were exploited for large-area device fabrication. An example is the coating of a commercial 365 nm UV-lamp (surface area of 125 cm^2) with the soft-hybrids that glowed bright white color when the lamp was connected to the electrical power (Figure 4D).

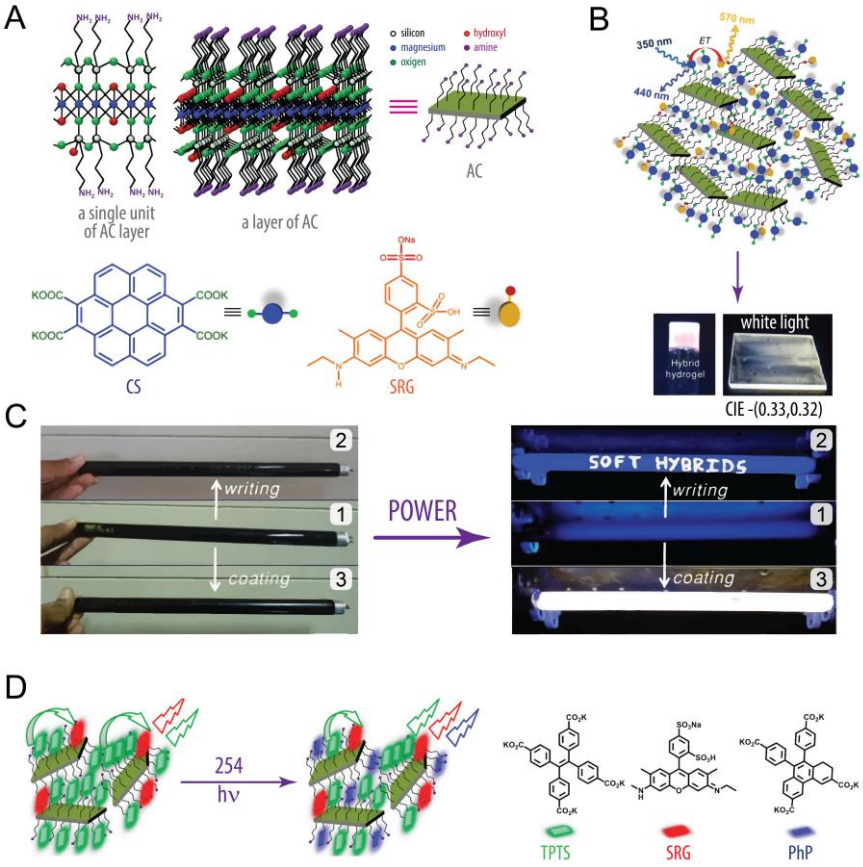

Figure 4. A) Molecular structures and schematic representation of the organo-functionalized clay and organic chromophores. B) Proposed schematic representation of the co-assembled AC-CS clay-chromophore soft-hybrids and the energy-transfer process to the acceptor red-emitting SRG molecules. Photographs of the white-light-emitting hybrids in gel and film phases are also shown. C) Schematic showing the strategy for photo-modulation of the clay hybrids. D) The hybrids were used to paint and write on commercial UV-lamps (365 nm) 1) uncoated lamp, 2) written as 'SOFT HYBRIDS' on the surface of the lamp and 3) lamp fully coated with the soft-hybrids. Hybrid-coated lamps are exposed to the UV irradiation by glowing lamps, which showed bright white light for both written letters and the fully-coated lamp. Taken with permission from references [66, 68]. Copyright (2013) Wiley-VCH.

QDs are also used as light-emitting centers in WLEDs, although typically the host framework is a polymer (e.g., polyfluorene, PFO, or poly(phenylene vinylene)-PFO copolymers) and not an organic-inorganic hybrid.[69, 70] A recent illustrative example is the embedding of yellow-, orange- or red-emitting QDs into a polyfluorene composite (called Green B). WLEDs with luminous efficiency > 17.2l m/W, correlated color temperatures of 3500 and 5500 K and high-color-rendering index (CRI up to 90 at 3500 K) were fabricated.[71] Nanocomposites of CdS QDs and silica-based carbon dots (CDs) were also proposed for WLEDs. An illustrative example are the hybrids emitting bright white light under UV excitation formed by the co-hydrolysis of blue fluorescent CDs functionalized by (3-aminopropyl) triethoxysilane (APTES) with yellow-emitting CdS nanocrystals modified by (3-mercaptopropyl) trimethoxysilane (MPTMS). A WLED was fabricated by the as-prepared CD/CdS QDs hybrids as converters, which exhibits white light with a color coordinate of (0.27, 0.32).[72]
Highly efficient WLEDs can also be fabricated with inorganic or organic-inorganic hybrid nanoparticles. A very intriguing example was reported by Ferreira *et al.* in 2014[73] in which WLEDs were produced by combining a commercial UV-LED chip (InGaAsN, 390 nm) and boehmite(*γ*-AlOOH)-based organic-inorganic hybrid material as white down-converting phosphor (**Figure 5A**). The hybrid organic-inorganic nanoparticles consist of few-nm thick boehmite nanoplates capped with *in situ* formed benzoate ligands prepared by a one-pot non-aqueous reaction (Figure 5B). The efficient white light emission results from a synergic energy transfer between the triplet level of the organic-phase (benzoate ligands, T_1) and the triplet state of the inorganic component (bohemite F-centres, ^3P). The efficient energy transfer results from two main aspects: i) the near-resonance between the T_1 and ^3P states and the ii) large spin-orbit effect that induce a high triplet radiative rate at room-temperature due to the presence of Al atoms coordinated to the benzoate groups. As a direct result of these two effects, the overall quantum yields of the boehmite hybrid nanoparticles are the highest reported so far for ultraviolet-pumped white phosphors. The WLEDs are able to emit white light with “Commission International de l’Éclairage” coordinates, color-rendering index and correlated color temperature values of (0.32, 0.33), 85.5 and 6111 K, respectively; overwhelming state-of-the-art single-phase UV-pumped WLEDs phosphors. We note that an important advantage of these boehmite hybrid phosphors lies in the fact that they are made of non-toxic, abundant and low-cost materials that is desirable from an industrial and environmental viewpoint.

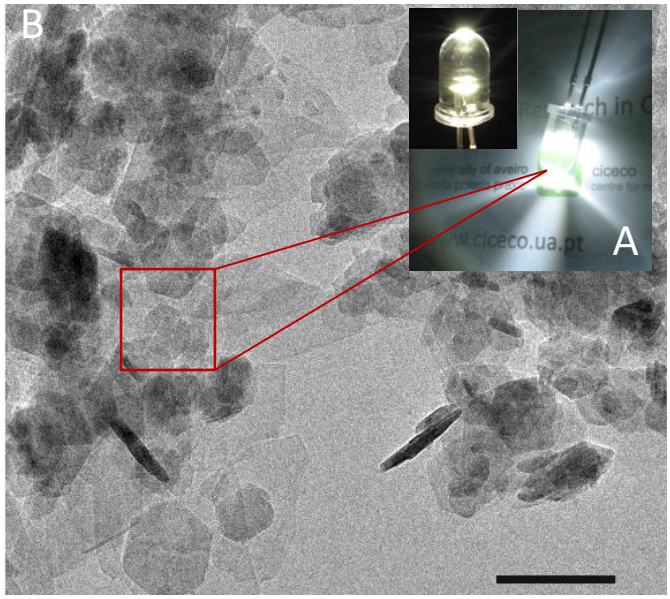

Figure 5. A) Photographs of the as-fabricated WLED using boehmite-based organic-inorganic hybrid nanoparticles operating at 3.0V. B) Representative TEM image of the boehmite hybrid nanoparticles (scale bar, 100 nm).[73]

Lanthanide-bearing organic–inorganic hybrids were also proposed for WLEDs. One of the first examples reported the fabrication of WLEDs by convening near-UV LED emission (390-420 nm) with a hybrid phosphor comprising two strontium aluminates, $SrAl_2O_4:Eu^{2+}$ (green emission) and $Sr_4Al_{14}O_{25}:Eu^{2+}$ (blue emission), and $Eu(btfa)_3phen$ (red emission), where $btfa^-$ = 4,4,4-trifluoro-1-phenyl-1,3-butanedionate and phen is 1,10-phenanthroline.[74]
A distinct approach involves the deposition of blue-, green and red-emitting organic-inorganic hybrid materials as homogeneous and transparent thin films (*ca.* 50 nm). In the example reported by Huang *et al.*, a sol-gel-derived hybrid showing emission from the blue to the yellow-green in a wide range of excitation wavelengths (254-380 nm) was synthesized with poly(9,9-dihexylfluorene-alt-9,9-dioctylfluorene) embedded into a silica matrix (blue-emitting component) and Tb^{3+} and Eu^{3+} ions coordinated in the matrix (green- and red-emitting components, respectively). Although white light was obtained for excitation at 340 nm, only the Eu^{3+} material was investigated as a potential phosphor coated on an UV LED.[75]
WLEDs were also fabricated using lanthanide-bearing metal organic frameworks (MOFs) through a remarkable methodology. Eu^{3+} ions were first encapsulated into MOF-253 using a post-synthetic method. The uncoordinated bipyridyl group of MOF-253 is ideal for chelate and sensitize the Eu^{3+}ions. The resulting MOF was further modified with tta (tta=2-thenoyltrifluoroacetone) and functionalized with ethyl methacrylate to achieve transparent polymer-MOF hybrid materials (MOF–PEMA-3.5) through radical polymerization. Finally, the polymer-MOF hybrid is assembled on a near-UV GaN chip to fabricate near-UV WLED (**Figure 6**) operating at 350 mA with a CCT of 3742 K and a CRI of 87.34.[76]

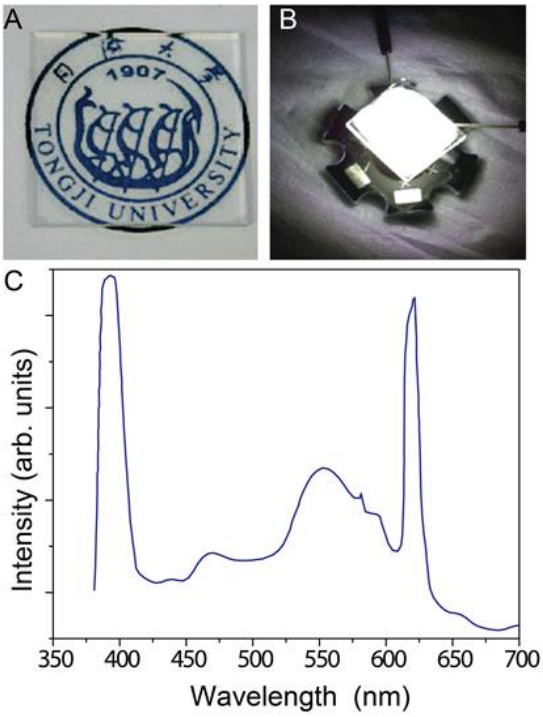

Figure 6. A) A photograph of MOF–PEMA-3.5 hybrid materials. B) The hybrids bright white light emission under excitation by a 395 nm GaN chip and C) the corresponding LED electroluminescent spectrum. Taken with permission from reference [76]. Copyright (2014) RSC.

Monochromatic LEDs were also fabricated based on dye-bridged hybrids[14-17] and Ln^{3+} complexes.[77] Concerning the former, an illustrative example is the functionalization of silsesquioxane cores with pyrene and 4-heptylbenzene that produced green emitting LEDs.[14] The resulting amorphous materials offer numerous advantages for OLEDs, *e.g.*, high glass transition temperatures, low polydispersity, solubility in common solvents, and high purity via column chromatography. The devices are among the highest efficient OLEDs fabricated up to now with fluorescent silsesquioxane, characterized by a high-external quantum efficiency of 3.64% and a luminous efficiency of 9.56 $cd \cdot A^{-1}$.[14]
With Ln^{3+} complexes, an interesting example involves the Eu^{3+}-bearing poly(MMA-MA-co-$Eu(tta)_2$phen) copolymer, where MA and MMA stand, respectively, for maleic acid and methyl methacrylate. A red-emitting LED was fabricated by combining the Eu-copolymer (quantum yield of 24% under near-UV light excitation) with a 395 nm-emitting InGaN chip.[77]

2.3 Random and feedback lasers

Interesting applications of dye-doped organic inorganic hybrids are random and distributed feedback lasers. A random laser is an open source of stimulated emission comprising a number of phenomena related to the emission of light by spatially inhomogeneous disordered materials (not bounded by any artificial mirrors).[78, 79] Laser emission is produced by multiple scattering processes that increase the dwell time of photons inside the material allowing amplification and creating gain saturation.[80] Random lasers were engineered to provide low spatial coherence and to generate images with superior quality than images generated with spatially coherent illumination.[81, 82] By providing intense laser illumination without the drawback of coherent artefacts (as those produced by lasers and superluminescent diodes that corrupt image formation), random lasers are well suited for full-field imaging applications, such as full-field microscopy and digital light projector systems.[82]
With organic-inorganic hybrid materials, examples comprise ZnO nanoparticles dispersed into a polymer matrix,[83, 84] Rh6G-doped SiO_2 nanoparticles,[78, 85] Rh6G-bearing di-ureasils,[37, 80] polymer films embedded with silver nanoparticles[86] and poly(2-hydroxyethyl methacrylate) (pHEMA) incorporating silsesquioxane nanoparticles (POSS) doped with the LDS722 and LDS730 red-emitting dyes.[87, 88]
Focusing on the example of Rh6G-bearing di-ureasils, the emission features of the ground powders were compared with those of a silica gel containing Rh6G-doped SiO_2 nanoparticles revealing a slightly larger slope efficiency and a lower threshold for laser-like emission in the later case (**Figure 7**).[37, 78] However, it is worth to note that these random laser performances (threshold and efficiency) in the di-ureasils have been obtained with a Rh6G concentration four orders of magnitude lower than the one used in the silica gel which makes the di-ureasil hybrids far more attractive for applications.[37]

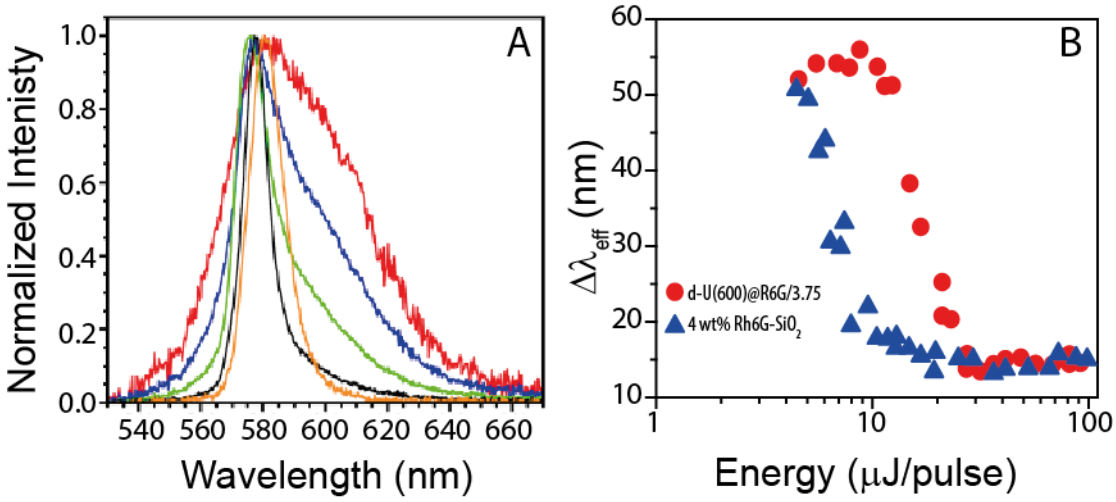

Figure 7. A) Normalized emission spectra of the ground powder of Rh6G-bearing di-ureasils obtained at 11 μJ/pulse (red), 18 μJ/pulse (blue), 20 μJ/pulse (green), 24 μJ/pulse (black), and 100 μJ/pulse (orange). B) Spectral narrowing of the ground powders of the di-ureasil hybrid (red dots) and the bulk silica gel (blue triangles). Taken with permission from reference [37]. Copyright (2010) OSA.

Distributed feedback (DFB) laser effect was also reported with dye-doped organic-inorganic hybrid materials, comprising polymers,[89, 90] biopolymers (such as silk fibroin[91]) and di-ureasils.[92] DFB lasers are devices operating in longitudinal single-mode oscillation due to a grating structure existing throughout the gain medium, providing the feedback for lasing, with potential applications in medical diagnosis and communications.[91] The nanofabrication capability of hybrid materials together with their superior physical, thermal, and optical properties, compared with those of isolated dyes, open up the possibility of using them as an alternative source for photonic devices, including random and DFB lasers.

2.4 Luminescent solar concentrators

Luminescent solar concentrators (LSCs) are cost-effective components easily integrated in photovoltaics. Despite the first reports date from 1976,[93, 94] LSCs reappeared in the last decade as an effective approach to collect and concentrate sunlight in an economic way, enhancing solar cells' performance and promoting the integration of photovoltaics architectural elements into buildings, with unprecedented possibilities for energy harvesting in façade design, urban furnishings and wearable fabrics.[95-100] Conventional LSCs are optical plastic waveguides doped with phosphors (*e.g.*, organic dyes, QDs, metal halide nanoclusters, or Ln^{3+} ions), or glass transparent (or semi-transparent) substrates coated with optically active layers embedding those phosphors. When exposed to direct and diffuse sunlight, part of the absorbing radiation is re-emitted at longer (downshifting or down-conversion) or shorter (up-conversion) wavelengths. Part of the emitted light will be lost at the surface and the rest will be trapped within the waveguide, or the substrate, and guided, through total internal reflection, to the edges, where it will be collected and converted into electricity by conventional photovoltaic cells (**Figure 8A-C**).

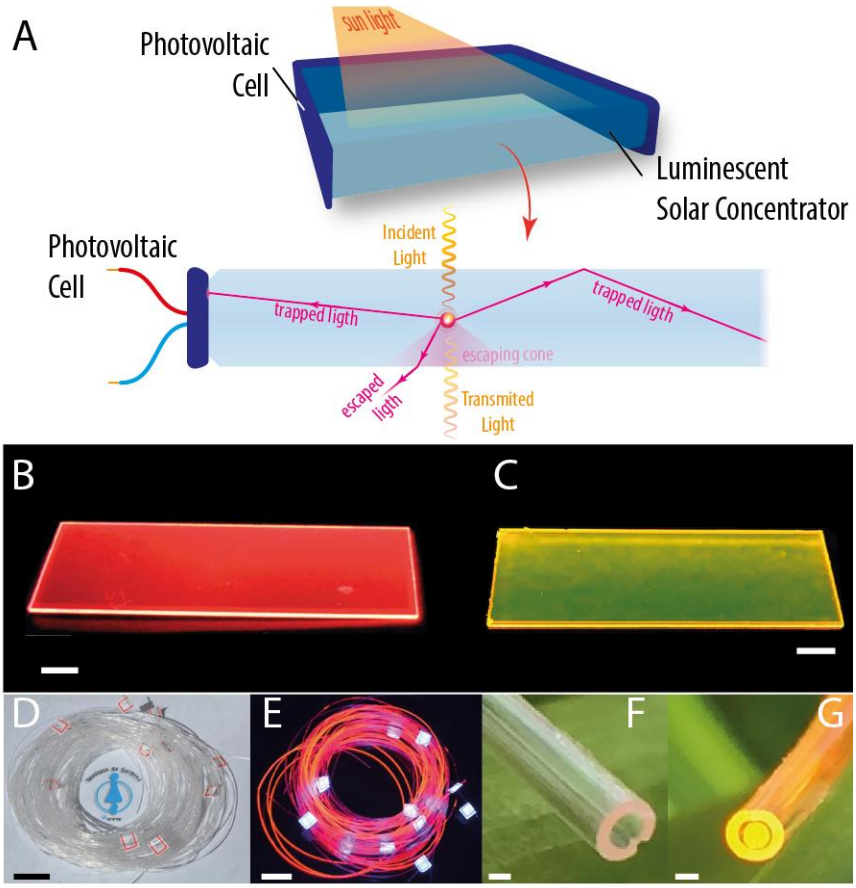

Figure 8. (A) Schematic representation of the working principle of a LSC. Photographs of two LSCs under UV irradiation (365 nm) based on (B) a di-ureasil hybrid doped with $[Eu(btfa)_3\text{-}(MeOH)_2]_2bpta_2$, ($bpta^-$ = trans-1,2-bis(4-pyridil) ethane and MeOH = methanol) and (C) a tri-ureasil hybrid doped with PTMS (phenyltrimethoxysilane) and Rh6G. Photographs of meter-length Eu-based di-ureasil LSCs under (D) daylight conditions and (E) UV irradiation (scale bars of 10^{-2} m). Detailed view of the Eu- (F) and Rh6G-based (G) LSCs extremities under outdoor illumination highlighting the light concentration (scale bars of 10^{-3} m). Taken with permission from reference [101]. Copyright (2016) RSC.

The research in LSCs has been displayed a substantial increase over the past three decades, with the major advances of the field highlighted in several recent reviews.[95-100] The development of LSCs faces numerous challenges, many of which related to the materials used, particularly related to the loss mechanisms that limit conversion efficiency (*e.g.*, emission quantum yield, reabsorption losses, incomplete utilization of the solar spectrum, and escape cone losses) and long-term photostability.[102] Various authors (even since the very beginning of the field[103]) concluded that it is unlikely that a single (organic or inorganic) material can overcome these issues, and organic-inorganic hybrids should play a key role on the LSC design optimization.[99, 102, 104] Moreover, despite the quite limited use of hybrid materials in the fabrication of LSC, their efficiency values are of the same order of magnitude as those of pure organic LSCs.[100] Recent examples of hybrid materials used in LSCs comprise polymers doped with QDs,[105, 106] metal halide nanocluster blends[107] and organic dyes,[104] Eu^{3+}-based bridged silsesquioxanes,[108-110] and di- and tri-ureasils doped with organic dyes and Eu^{3+} β-diketonate complexes.[101, 111-113]

An intriguing example of lightweight and mechanically flexible high-performance waveguiding photovoltaics is the fabrication of cylindrical LSCs of plastic optical fibers

(POFs) coated (bulk fibers) or filled (hollow-core fibers) with Rh6G- or Eu^{3+}-doped organic–inorganic hybrids (Figure 8D-G).[101, 112] Cylindrical LSCs have a large potential compared with that of planar ones, despite the very small number of examples involving short length (10^{-2} m) bulk or hollow-core POFs that can be found in the literature.[114-116] First, the concentration factor *F* (that dominates the devices' performance) of a cylindrical LSC can be twice higher than that of a square-planar one of equivalent collection area and volume.[117] Second, the cylindrical geometry allows an easier coupling with optical fibers that could transport light to a remote place for lighting or power production and renders easier photovoltaic urban integration.[101] In the example illustrated in Fig. 8, a drawing optical fiber facility is used to scale up de area of the devices demonstrating the possibility of obtaining large area LSCs (length up to 2.5 m) based on bulk-coated and hollow-filled POFs with unprecedented concentration factors, up to 11.75.

2.5 Luminescent thermometers

The already mentioned unique characteristics of organic-inorganic hybrids, in particular their capability to incarcerate luminescence organic and inorganic thermometric probes (*e.g.*, organic dyes, QDs and Ln^{3+} ions), preventing the aggregation and the emission degradation, makes them suitable for the design of thermometric systems. Moreover, the combination of organic and inorganic counterparts can also induce synergic effects resulting in an enhancement of the thermometric efficiency, relatively to that of the organic or inorganic thermometric probes alone, and multiplying the design possibilities of luminescent micro and nanothermometers.[118] Luminescent thermometry exploits the temperature dependence of the light emission features of the thermometric probes, namely emission intensity,[119-121] peak position,[122] and excited-states lifetime[123, 124] or risetime,[125, 126] possessing the unique advantage of high-resolution contactless measurement, even in harsh environments and under strongly electromagnetic fields.[127-130] Although relatively recent (luminescent thermometry exploded over the past five years), the technique appears to be beneficial to many technological applications in a great variety of areas, such as microelectronics, microfluidics, bio- and nanomedicine.[131]

Examples of luminescent thermometers based on organic-inorganic hybrids include metal-organic molecular compounds,[132] layer double hydroxides,[133] metal-organic frameworks,[134] polymer nanocomposites,[135] QDs in polymers,[136] inorganic NPs coated with an organic (or hybrid) layer,[137] and di-ureasil films co-doped with Eu^{3+} and Tb^{3+} β-diketonate complexes.[119, 138] These later films were used as self-referenced and efficient luminescent probes to map temperature in microelectronic circuits[119, 138, 139] and optoelectronic devices,[140] demonstrating an intriguing application of hybrid materials in microelectronics. The thermal gradients generated at submicrometer scale by the millions of transistors contained in integrated circuits are becoming the key limiting factor for device integration in micro- and nanoelectronics and, then, non-contact thermometric techniques with high-spatial resolution (such as luminescent thermometry) are essential for non-invasive off-chip characterization and heat management.[141] The diureasil films incorporating $[Eu(btfa)_3(MeOH)(bpeta)]$ and $[Tb(btfa)_3(MeOH)(bpeta)]$ complexes allowed temperature mapping in wired-board circuits and in a Mach-Zehnder interferometer using commercial detectors and excitation sources.[118, 138, 140] For instance, **Figure 9** shows temperature profiles of a FR4 printed wiring board reconstructed from the emission spectra of the Eu^{3+}/Tb^{3+}-containing di-ureasil. The higher spatial resolution obtained, 0.42 μm, is 4.5 times lower than the Rayleigh limit of diffraction (1.89 μm) in the experimental conditions used, and much lower than that recorded with a state-of-the-art commercial IR thermal camera (~130 μm). As the temperature readout results of a spectroscopic measurement it is not limited by the Rayleigh criterion and, thus, the spatial resolution is only limited by the experimental setup

used that produces a field-of-view averaged temperature change above the sensitivity of the detector.[138] The measured temporal resolution is of the order of the integration time of the detectors used (5-100 ms). Although there is not a single technique able to combine sub-micron and sub-millisecond resolutions, up to now, the examples that have the best performance are those based on luminescent Ln^{3+}-doped organic-inorganic hybrid thermometers.

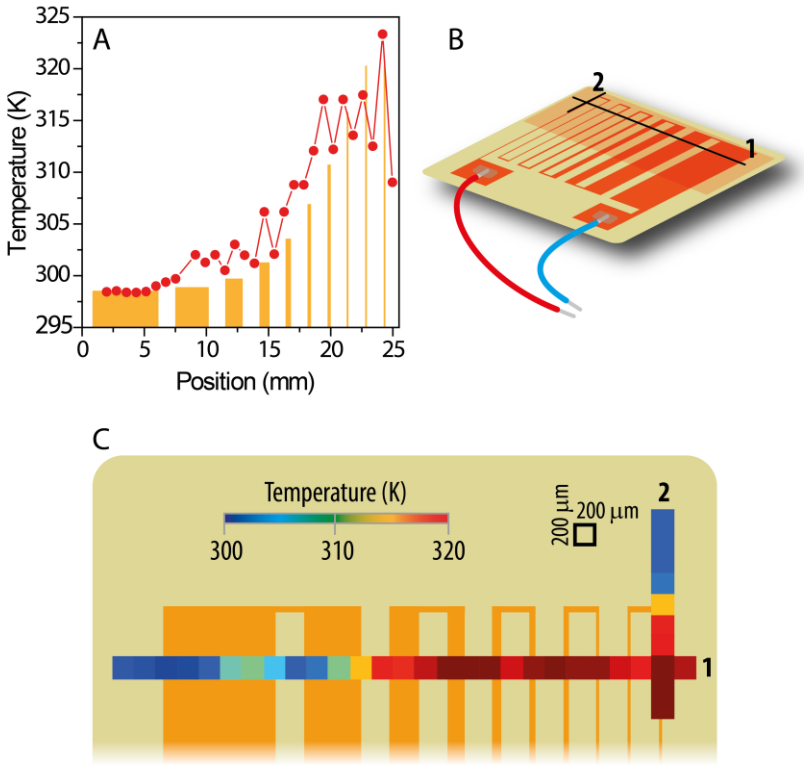

Figure 9. (A) Temperature profile obtained with a Eu^{3+}/Tb^{3+} co-doped di-ureasil film of the FR-4 wire-board depicted in (B). The emission of the film (excited at 365 nm) is collected with a 200 µm core diameter fiber along the direction denoted by 1 using a scanning step of 200 µm. The temperature uncertainly is 0.5 K. The orange shadowed areas correspond to the distinct copper tracks. (C) Pseudo-color temperature maps reconstructed from the emission of the di-ureasil along the two perpendicular directions denoted by 1 and 2 of the FR4 printed wiring board.

3. Photochromic hybrid materials

3.1 Introduction to photochromism

According to the International Union of Pure and Applied Chemistry (IUPAC)[142] definition, *photochromism* is "a reversible transformation of a chemical specie induced in one or both directions by absorption of electromagnetic radiation between two forms, A and B, having different absorption spectra". The thermodynamically stable form A is transformed by irradiation into form B, and the back reaction can occur thermally (*T-type photochromism*) or photochemically (*P-type photochromism*). In most cases, a change in color towards longer wavelengths absorption takes place (*positive photochromism*). However, when λmax(A) > λmax(B), photochromism is called *negative or inverse*. **Figure 10** summarizes the concept of reversible photochromism.

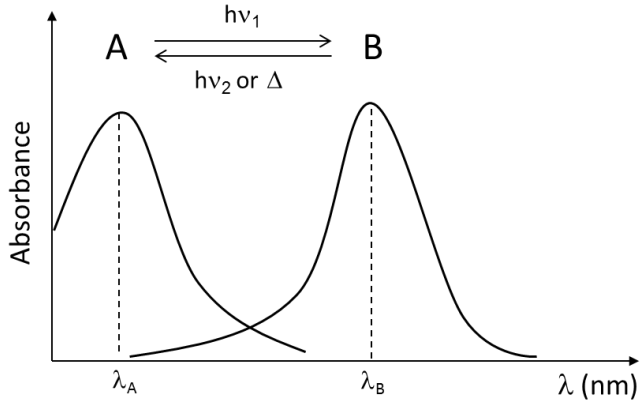

Figure 10. Reversible photochromism. Adapted with permission from ref [142]

This interconversion between two states is accompanied by the change of color but also change in refractive index, dielectric constant, redox potentials, solubility, viscosity, surface wettability, magnetism, luminescence, or a mechanical effect. Therefore, besides the well-established use of photochromic materials in ophthalmics (lenses for sunglasses), there is a growing list of other real or potential application areas, including cosmetics, security, displays and filters, optical memories, photo-optical switches, photography, photometry, and so on.

There are many types of chemical species exhibiting photochromism. Most of them are organic molecules, which are able to absorb one photon (*one-photon mechanism*) to form B from the singlet (1A*) or triplet (3A*) excited states, or to absorb two photons (*two-photon mechanism*) where B is formed from the population of an upper excited state. The main families of organic photochromic compounds are spiropyrans (SP), spirooxazines, chromenes, fulgides, diarylethenes, dithienylethene, spirodihydroindolizines, azo compounds, polycyclic aromatic compounds, anils, polycyclic quinones, viologens, triarylmethanes, and biological receptors as retinal proteins and phytochrome. The chemical processes usually involved in the organic photochromism are pericyclic reactions, cis-trans (E/Z) isomerizations, intramolecular hydrogen/group transfers, dissociation processes and electron transfers.

In contrast to organic molecules, photochromic inorganic compounds are comparatively few. They include metal halides of group IB metals (such as silver halides), oxides, polyoxometalates and carbonyls of VIB transition metals (i.e. WO_3, MoO_3), oxides of group IVB and VB metals (TiO_2, V_2O_5, Nb_2O_5…), zinc sulfide, alkali metal azides, sodalite, mercury salts, Ni–Al layered double hydroxides, valence-tautomeric Prussian blue analogs and so on. The origin of the color change is the ability of these compounds to change stoichiometry, and their performance is related to electron/hole pairs interacting with their environment (air, liquid solution, adsorbed water or solvent molecules, rigid matrices, etc.). Thus, the photochromic properties show a critical dependence on the surrounding medium, which is often hard to predict and systematize.

For a more detailed accounts on the classical photochromic phenomenon, materials and applications we invite the readers to consult the books edited by Crano and Guglielmetti,[143, 144] Bouas-Laurent and Durr[145], or Bamfield and Hutchings[146].

The research on photochromic systems from the individual organic or inorganic fields has been very difficult. Organic–inorganic hybrid (OIH) photochromic materials can be extremely versatile in terms of physical and chemical properties, compositions, and processing techniques. Thus, they offer a wide range of possibilities to fabricate tailor-made photochromic materials in which the final response will depend not only on the chemical nature of each component but also on the interface and synergy between both organic and inorganic counterparts. The adequate design of OIH allows: (i) to improve photophysical and

photochemical properties (especially via molecular modification in organic chromophores), (ii) to offer easy-to-shape materials for a real commercial deployment (via integration of the active species into functional matrices) and (iii) to explore new photoresponsive multicomponent systems. Excellent reviews have been written by J. Yao,[147] G. C. Guo[148] and D. Levy.[149, 150]

But their economic potential is still not being fully realized due to the difficulty to simultaneously fulfill some relevant technical requirements for application. Some of them are:

1. The material must develop a strong color rapidly upon UV/vis irradiation.
2. The fade rate back to the colorless state must be controllable.
3. The response must be constant through many coloration cycles.

In the last decade, great efforts have been devoted to accomplish these issues but for some applications the achievements are still far from a real implementation. Also, the choice of the system and the specific requirements depend on the targeted application. In sunglasses or protective coatings, for instance, the consumer needs robust systems with an immediate reaction to a change of external conditions. Also, a change from white (or colorless) to grey or even black is preferred, especially for large-volume displays (display panels, front and rear windows, and mirrors for cars and trucks…). For other applications, multicolored systems can be desirable. Indeed, most of the photochromic compounds do changes between two or more different colors, and that is useful for sensors or markers. For memories, data storage or switches, for instance, a good contrast between the two states is probable the most valuable property. Here, we give a brief overview of the most recent progress in this area, focusing on photochromic hybrids where photochromism comes mainly from organic molecules, from inorganic species or combination of both. Their applications will be progressively presented and discussed in terms of their structural and physicochemical features.

3.2 Organic photochromism in hybrids

Organic photochromism offers several tens of thousands of molecules with which one can tailor their applicability by the shade of color change, the direction of the photochromism, the rate of change in color intensity, reversibility, etc. To achieve robust and functional photochromic-based devices that could be easily handled and integrated in solid materials, the main approach followed is the micro-/nano-structuring of photochromic molecules into organic-inorganic hybrid materials (classical sol-gel glasses, polymers, nanoparticles, etc…) via weak (*Class I* hybrid)[31] or strong (*Class II* hybrid) chemical interactions.[151-165] Among the photochromic organic molecules, spirooxazines, azobenzenes, diarylethenes and fulgides have been the most extensively studied.[144] These molecules can easily be entrapped in ORMOSIL (Organically Modified Silanes) hybrid matrices.[166] A huge work was done on this area in the late 90's and early 2000's with the boom of *Soft Chemistry*.[167] The synthesis of these matrices involves inorganic polymerizations at room temperature from metal-organic precursors, so under these mild conditions, the active molecules can be stored preserving or improving their photochemical and photophysical properties. The main advantages of silane matrices over pure organic polymers (PMMA, PAA…) are the higher thermal stability and the possibility of chemical modification that can be of interest for a particular application (for instance, including specific functional groups or changing properties like refractive index, the hydrophilic/phobic character, etc.). This approach is also more convenient than obtaining photochromic single crystals.[168-170] Few organic molecules preserve their photochromic properties in the solid state[171], but even so the shaping and conformation into practical devices is really difficult. In the last years, extended literature can still be found on photochromic dyes randomly embedded (covalently bonded or just doped) into amorphous hybrid silica derivates (nanoparticles,[172] films,[173] fibers,[174]) and also in layered

materials.[175] As a difference to classical works, the more recent articles deal with the combination of photochromic properties to other functionality to get multifunctional systems. For instance, J. Fölling[172] have designed a new functional (amino reactive) highly efficient fluorescent molecular switch (FMS) with a photochromic diarylethene and a rhodamine fluorescent dye on silica nanoparticles, with application in fluorescent microscopy (**Figure 11 (a)**). Other works are devoted to develop new procedures of shaping and conformation, such as the fibers shown in Figure 11 (b).

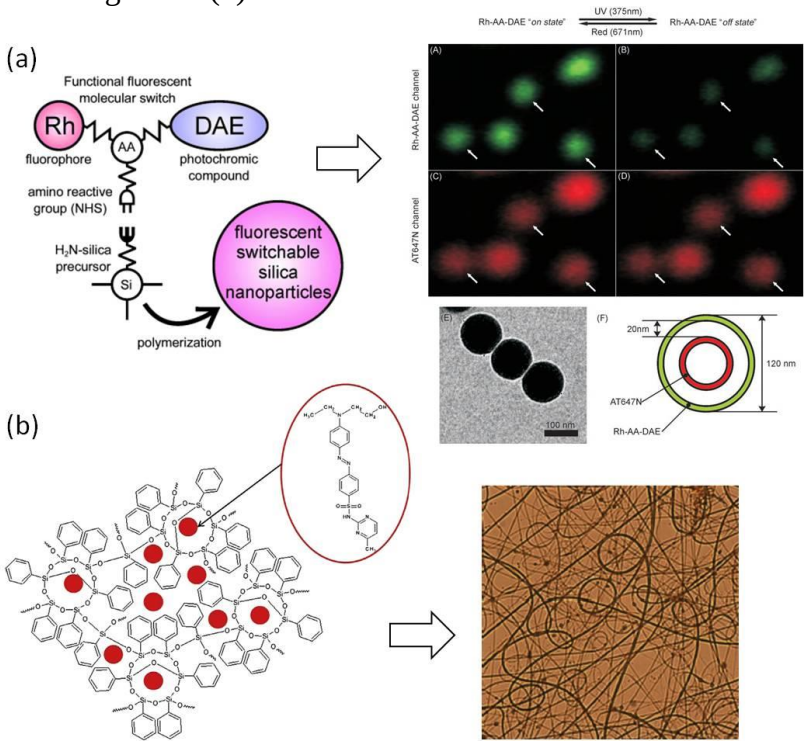

Figure 11. *(Top)* Chemical structure of the fluorescent molecular switch Rh-AA-DAE and the photochromic reaction responsible for the fluorescence modulation. The fluorophore moiety is excited with green light: red light is emitted in the on state, while resonant energy transfer prevents this emission in the off state. Confocal images of fluorescent NPs (120 nm) doubly stained with Rh-AA-DAE and AT647N, recorded in two channels. The lower panel shows a TEM image of the particles (E) and a scheme with the distribution of the dyes inside each particle (F). Adapted with permission from ref [172]. *(Bottom)* The guest-host system containing photoactive dye of SMERe incorporated into triethoxyphenylsilane matrix. SEM pictures showing the fibrous structure of the hybrid materials. Adapted with permission from ref [174].

An interesting idea to facilitate photochromic transformations is to include the organic dye into mesostructured materials with inorganic and organic domains separated at the nanometric scale. G.D. Stucky[176] reported a block-copolymer/silica nanocomposite used as host for two photochromic dyes, a spirooxazine and a spiropyran, where the dyes are incorporated predominantly within the hydrophobic occlusions. The materials exhibit direct photochromism with faster response times, being at that time in the range of the best values reported so far for solid-state composites. These silica/block-copolymers can also be processed easily in any desired shape, including fibers, thin films, monoliths, waveguide structures, and optical coatings. Similar systems based on spiropyrane doped PMMA-silica have been reported, in which the presence of PMMA reduces the polar character of the matrix, facilitates the solubility of the dyes, modify the stability of particular isomers, and increases the chemical durability of the hybrid (**Figure 12**).[177]

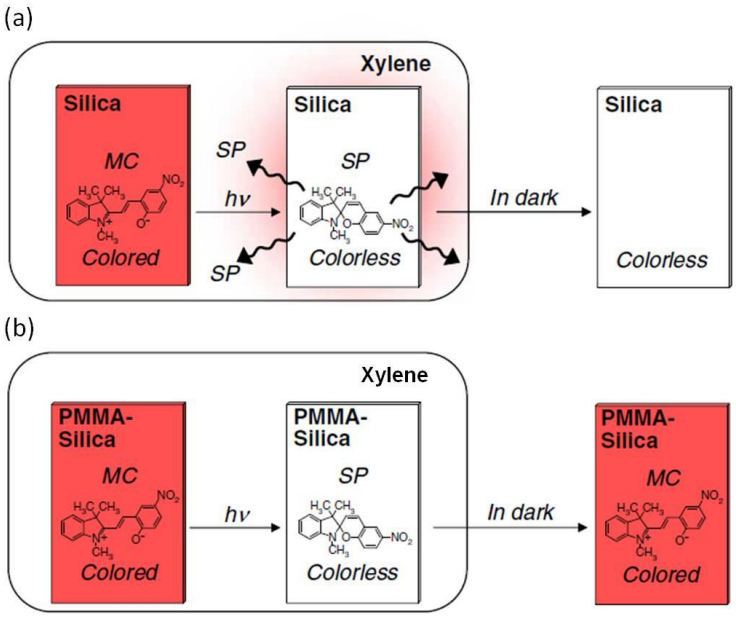

Figure 12. Schematic illustration on the changes in the state of spiropyran molecules during soaking in xylene for pure silica (a) and PMMA-silica (b) systems under visible light and in the dark. Adapted with permission from ref [177].

The rational design of the hybrid nanocomposite is of great importance because the dye-matrix interaction is responsible for a good chemical compatibility. Indeed, the main limitations in these materials are usually the low content of photochromic species, low photochromic conversions in the solid state, or alterations in the chemical structure of the isomers during the polymerization process. F. Ribot *et al.* demonstrated in spirooxazine-doped tin-based nano-building blocks (NBBs) embedded in PEG copolymers that the interfaces can be tuned to afford a fast photochromic response together with a high dye content.[178] Some publications have addressed this dye-matrix interaction to fully exploit the properties and tuneability of the photochromic hybrid systems. R. A. Evans *et al.*[179] reveal that the intramolecular interactions of flexible PDMS (poly-dimethylsiloxane) oligomers with the photochromic dyes make possible faster chemical processes, greatly increasing the dye switching speed in a rigid hybrid system such as PDMS ophthalmic lenses. Both coloration and fade behavior indicate that the spirooxazine 1 (**Figure 13**) is in a highly mobile, near solution-like environment within the rigid matrix The greatest impact was observed in the thermal fade parameters $T_{1/2}$ and $T_{3/4}$—the times it takes for the optical density to reduce by half and three quarters of the initial optical density of the colored state—which were reduced by 75% and 94% for this dye in a host polymer with a glass-transition temperature of 120 °C. This is a quite surprising result because bonding photochromic dyes to polymers in low concentrations usually slows down the switching process.[180] The key difference in the Evans' work is that a low Tg oligomer provides a localized favorable switching environment where it is needed, i.e. near/around the dye. Thus, the compatibility between the covalently bonded oligomer to the dye and the matrix allowed a greater molecular mobility for the switching process, which can find utility in data recording or optical switching.

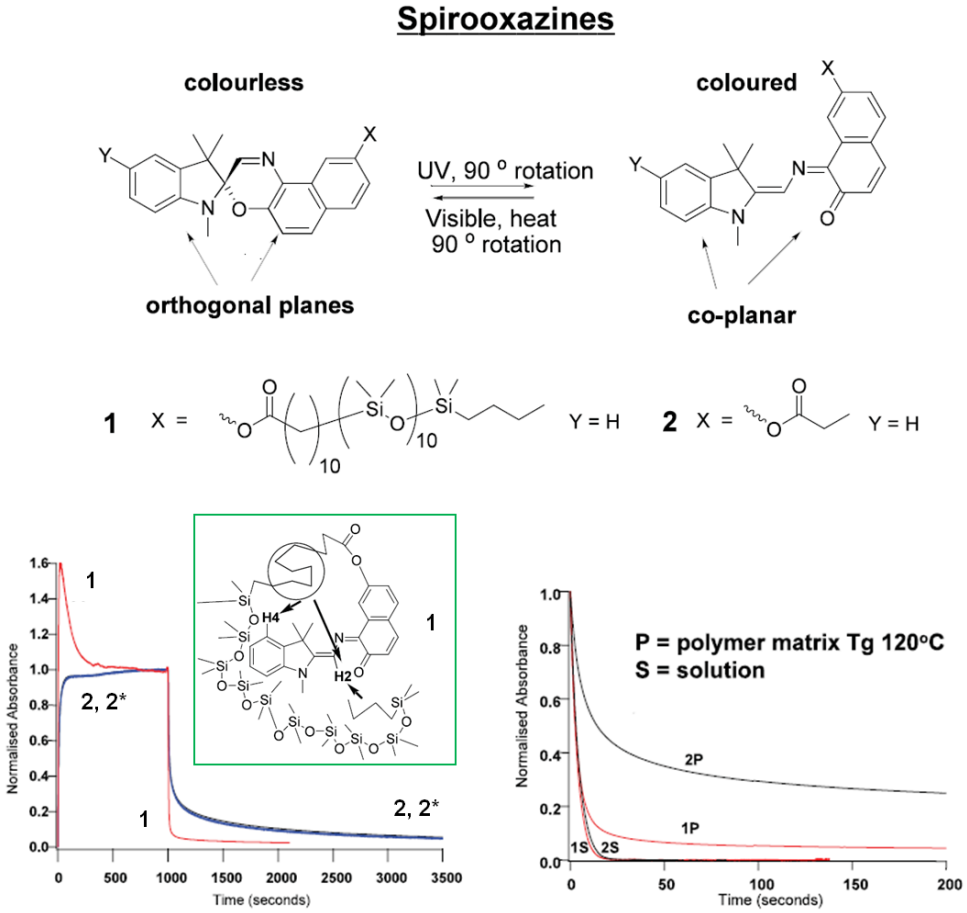

Figure 13. *Top:* Structural changes of spirooxazine compounds during photochromic switching. *Bottom left:* Positive effect of conjugating a spirooxazine (compound 2) with a short PDMS chain (compound 1) on coloration and decoloration speeds. The covalent bonding between dye and silane oligomer is crucial for increasing the transformation speed (compare compound 2 with 2*, where 2* is the spirooxazine with PDMS oligomers added to the matrix, without chemical bonding). The intramolecular interaction of PDMS units with dye is shown in a green square. *Bottom right*: The solution-like fade performance of compound 1 in the rigid silane matrix (curve 1P) as compared to 1 and 2 in toluene solution (curves 1S and 2S) and compound 2 in the identical rigid silane matrix (curve 2P). Adapted with permission from ref [179].

The rigid environment of a dye molecule within the hybrid matrix can be beneficial, for instance, to avoid a non-desired photochromic transformation. This fact is detailed in amine-alcohol-silicate hybrid materials doped with naphthopyran,[181] where the isomerisation of one specific colored isomer (which is a space demanding reaction) is hindered, and films present fast and fully reversible coloration/transparent cycles upon irradiation/dark (**Figure 14**). This behavior contrasts with the classical performance of naphthopyrans that generates two colored species, associated to two isomeric species, with different kinetics. In this case, the structural design prevents the formation of the long-lived colored specie, leading to faster and reversible photo-switchable materials.

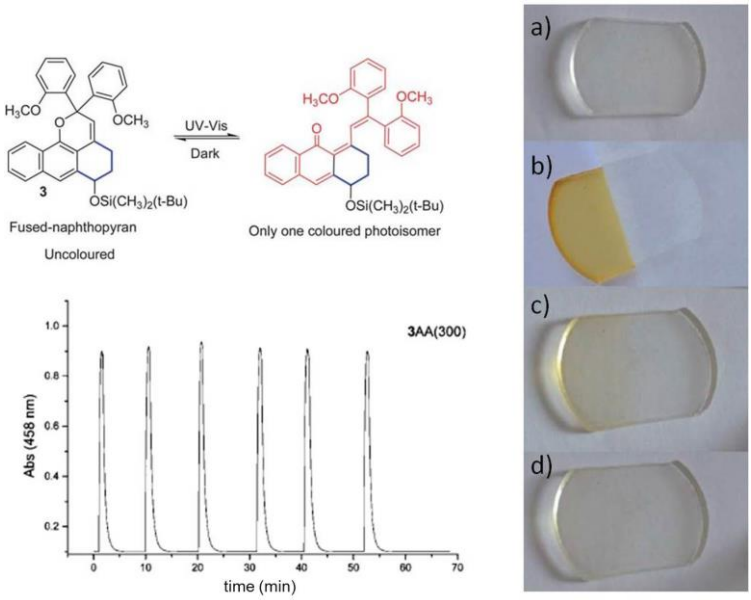

Figure 14. Photochromic equilibrium for the fused-naphthol[1,2-*b*]pyran. UV-vis irradiation/dark cycles of gels doped with naphthopyran 3 measured at 458 nm. Samples 3AA(300) in the dark (a), exposure of half of the sample to sunlight for 1 min (b), sample after 60s in the dark (c) and after 120s in the dark (d). Adapted with permission from ref [181].

Another interesting approach is to exploit the dye-matrix interaction to get periodically organized nanostructures through a *template effect*. Numerous studies about hybrids including viologen cations (1,1'-disubstituted-4,4'-bipyridinium, V^{2+} cations) use this effect. Viologens are electron-acceptor species that, in the solid state and upon irradiation, can accept one electron from a donor entity such as halides or pseudohalides X^- or a neutral molecule D, to afford stable separated charge state systems that find applications in electrochromic displays, molecular electronics, solar energy conversion, etc. N. Mercier published an excellent review showing peculiar interactions between viologen dications and anions of hybrid structures.[182] One pioneer result was found in (MV)[$MX_{5-x}X'_x$] ((M = Bi^{III}, Sb^{III}; X = Cl, Br, I; x = 0–5) compounds that exhibited ferroelectric properties thanks to the electron-donor interaction of a methylviologen dication with polar MX_5 chains of trans-connected octahedra (**Figure 15**).[183]

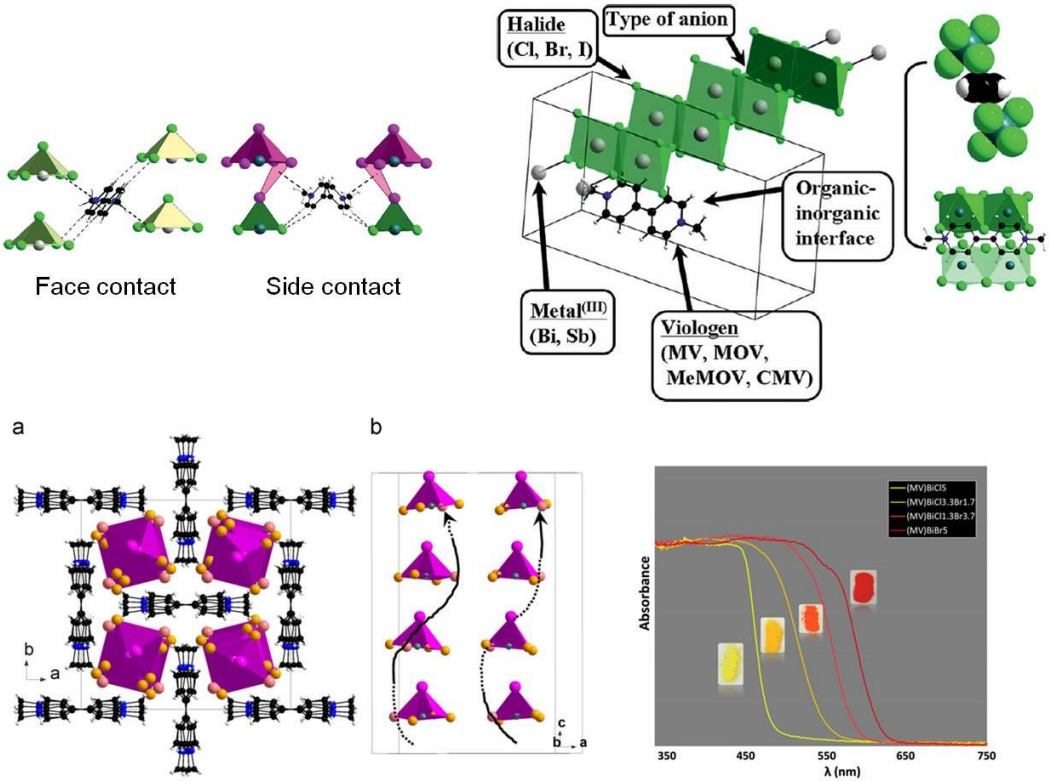

Figure 15. *Top:* (Left) Interactions at the organic-inorganic interface between one methylviologen cation and two anionic chains showing face and side contacts. (Right) Part of the structure of (MV)[Bi_2Cl_8] showing one methylviologen entity and the inorganic network (left) and interactions between the organic cation and two inorganic anions (right: side view in space-filling representation and viewed along the direction perpendicular to the viologen plane), and the different parameters that can influence the photoinduced charge-transfer process in viologen halometalate salts. Adapted with permission from ref [182]. *Bottom:* Structure of (MV)[$SbBr_{3.8}I_{1.2}$] viewed along the chain axis showing the tetragonal arrangement (a), and *syn* coupling of two neighbouring chains which displays opposite chiralities (b). UV-vis spectra and pictures of (MV)[$Bi_2Cl_{5-x}Br_x$] (x=0, 3.7, 5) hybrids. Adapted with permission from ref [183].

Asymmetric viologen ligands can be also coordinated to Zn(II) centers through a *template effect*, leading to the first example of bulk electron-transfer photochromic compound with intrinsic second-order nonlinear optical (NLO) photoswitching properties.[184] The electron transfer is possible thanks to the synergetic interaction between the ligand and a metal center with acentric coordination geometry. Briefly, the structure exhibits a 1D polar chain infinite structure with continuous head-to-tail linking of metallorganic units (one zinc atom linked to an acceptor viologen moiety and two electron donor species) that cross-stack according to the acentric space group (Cc), giving rise to the macroscopic polarization in the bulk (**Figure 16**).

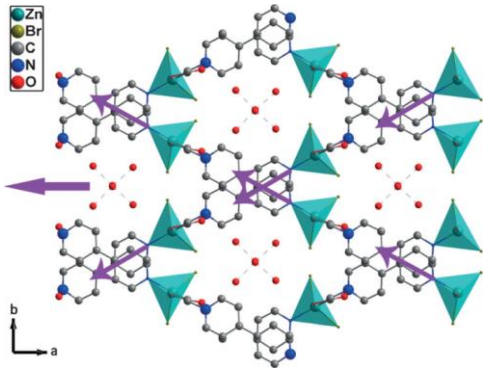

Figure 16. Molecular packing in a crystal of [$ZnBr_2$(μ-CEbpy).3H_2O] view along the c-axis. The violet arrows indicate the whole remnant polarity. Adapted with permission from ref [184].

The use of light as an external trigger to switch the second-order NLO activity has been increasingly addressed for nondestructive data storage or opto-optical switching in the emerging field of photonic devices.[185] However, there is a long way to use them in practical applications because of the low reaction speeds and the limited contrast for the photoswitching of NLO properties. To overcome these problems, M. Schulze et al.[186] propose the anchoring of photochromic fulgimide molecules into a self-assembly monolayer (SAM) on a Si(111) surface. The use of silicon, one of the most relevant materials for semiconductor devices, as a substrate for SAM formation and the further anchoring and aligning of molecular switches (photochromic molecules) paves the way for an efficient switching of the NLO response with higher contrast (**Figure 17**).

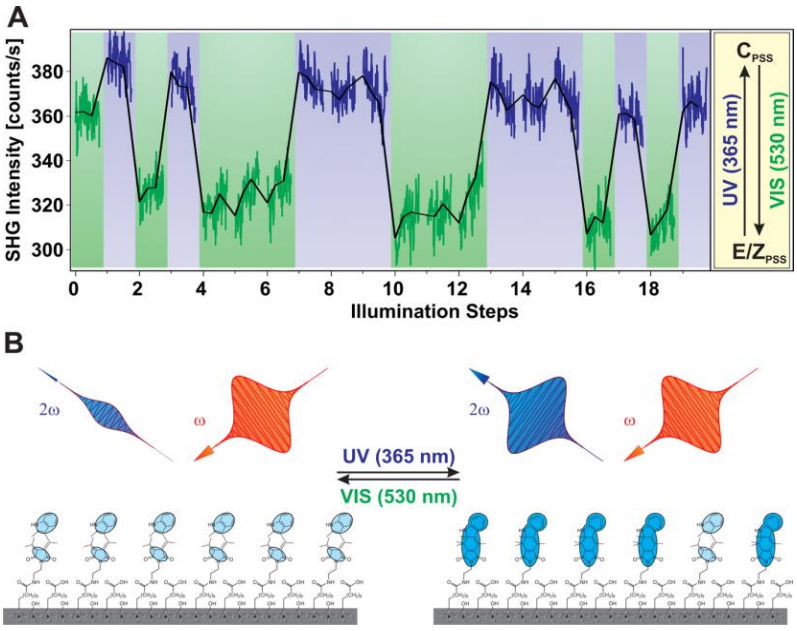

Figure 17. (A) Changes in the second harmonic generation (SHG) signal amplitude as a function of illumination with different wavelengths (365 and 530 nm), demonstrating the light-induced reversible changes in the NLO interfacial response due to the ring-opening/closure reaction. (B) Scheme of the reversible photoinduced switching probed with SHG. Adapted with permission from ref [185].

Periodically organized systems have demonstrated to enhance the photochemical processes over amorphous photoresponsive materials. Thus, the covalent grafting of organic molecules

(flavilium, spyropyrans, etc.) in different types of mesoporous matrices (MCM-41, SBA-15, polymers, and so on) has also been investigated. The ordered nanostructure and the strong dye-matrix bonding enhance their photostability and avoid leaching of the dyes. To mention some of the most interesting achievements, S. Gago[187] prepared a solid state pH-dependent photochromic material with fast kinetics in color change thanks to the highly ordered hexagonal arrays of channels in mesoporous silica.

More sophisticated designs, such as core-shell or hollow spheres[188] have also great interest. An example can be the smart nanocapsules reported by J. Allouche[189] that are made of a dense silica core with mesoporous photochromic (SP) silica shell in a dual templating sol-gel method. A different strategy is explored by J. Hernando and D. Ruiz-Molina[190] in which photochromic molecules are encapsulated into liquid-filled polyamide capsules to achieve high switching speeds in solid materials. The authors state that its strategy is universal and does not require synthetic modification of commercially available photochromes, what is of great interest for industry. Furthermore, the hollow structures provide photochromic solid materials with solution-like color fading kinetics, which are about one order of magnitude faster than those measured upon direct dispersion of the photosensitive molecules into rigid polymer thin films and solid particles.

Regarding non-silica systems, N. Andersson[191] synthesized ordered honeycomb porous films made of a spiropyran functional PAA polymers that shows a rapid and intense colour changes upon irradiation with UV and vis light. An attractive point is that these nanostructures can also entrap metal ions (Pt, Pd…) or nanoparticles that shift the absorption and the chromic response, acting as reversible metal ion sensors.[192] Complex architectures can be designed to make possible energy transfers between photochromic dyes and other luminescent species such as Quantum Dots[193], up-converting nanocrystals[194-196] or plasmonic metal nanoparticles[197, 198]. One nice example is the decoration of CdSe/ZnS QDs with an amphiphilic photochromic polymer coating[199]. The core-shell architecture permits the accommodation of hydrophobic acceptor dyes in a close proximity to the QD donor, thereby providing an effective FRET probe in a small (~7 nm diameter) water-soluble package (**Figure 18**) that opens up numerous applications in biological and live cell studies.

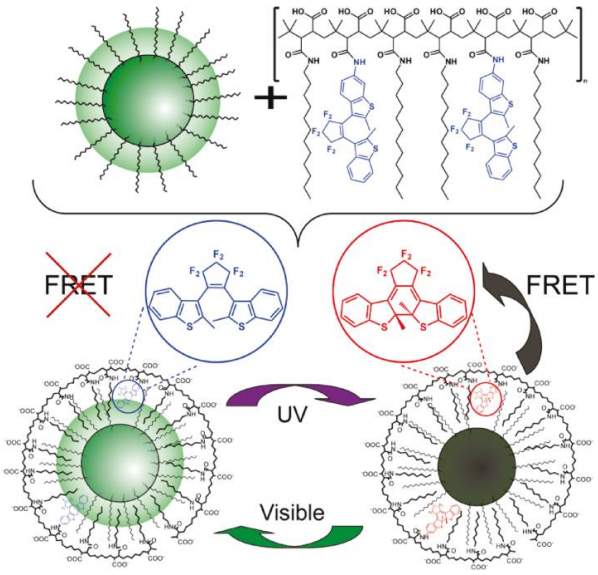

Figure 18. Photoswitching QDs coated with an amphiphilic photochromic polymer. The fluorescence of the psQD is toggled with FRET by modulating the absorbance of the photochromic polymer with UV and visible light. Adapted from reference [199].

Hybrid nanomaterials combining organic photochromes with plasmonic nanoparticles have also gained considerable interest in the fields of data storage, photovoltaics, biosensing, etc.[200, 201] The mutual interplay between organic molecules and metal properties can be used to finely tune the photochrome reactivity as well as the energy of the localized surface plasmon resonance (LSPR) of the metallic nanoparticles. In some cases, the light-induced photochromic process (for instance, photoisomerization between the *trans* and *cis* states in azobenzene molecules) results in significant changes in other properties like refractive index, with interest for optical switching and filtering. Most of the studies reported so far deal with grafted diarylethene[202] and spiropyrane[203] derivatives, characterized by an initial colorless state and a colored photoreacted state that causes an energy shift of the LSPR band in a privileged manner. P. A. Ledin[200] reports the fabrication of silver nanocubes coated with photochromic azo-silsesquioxane hybrid derivatives and deposited onto quartz substrates (**Figure 19** ***top***). The photochromic transformation induces variations in the refractive-index medium and a reversible tuning of the plasmonic modes of noble-metal nanostructures. Also, gold nanorods can be coated with silica and functionalized with grafted fluorescent and photochromic derivatives (Figure 19 *bottom*).[204] Spectroscopic investigations demonstrated that cross-coupled interactions between plasmonic, photochromic, and fluorescence properties play a major role in such nanosystems, depending on the thickness of the silica spacer, leading to multi-signal photoswitchability.

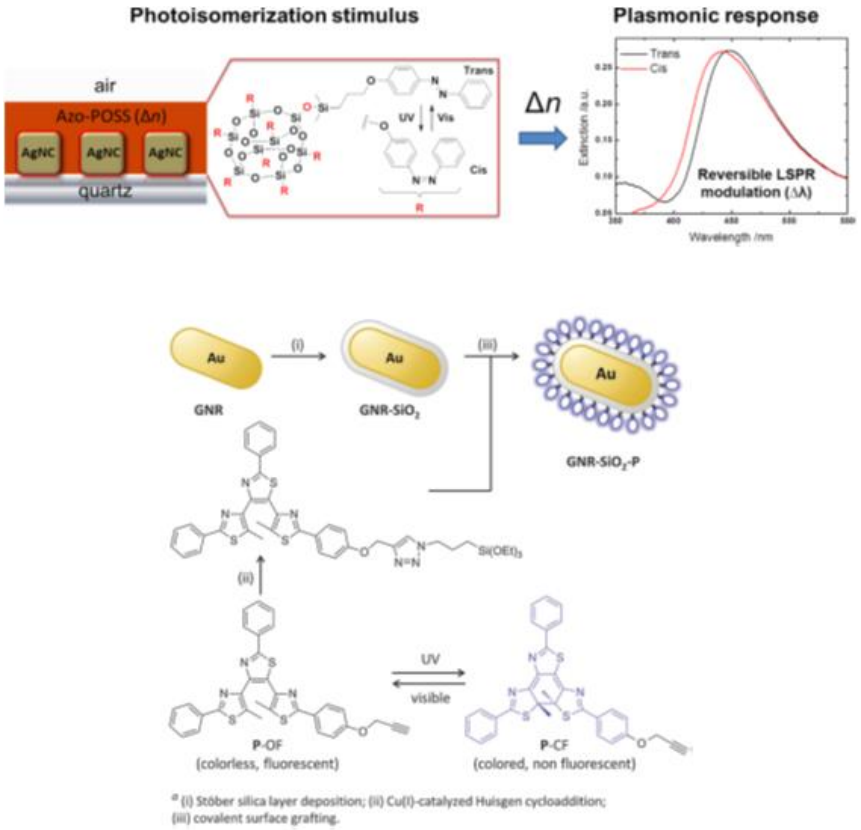

Figure 19. *Top:* Branched Azo-POSS conjugates as a variable-refractive-index matrix for plasmonic nanoparticles. Adapted with permission from ref [200]. *Bottom:* Synthesis of the silica-coated gold nanorods with surface grafted photochromic and fluorescent derivatives. Adapted with permission from ref [204].

Multicolored systems have been developed by embedding two or more active species in matrices. These materials can be used in multifrequency photochromic recording, multicolor displays, inks, barcodes, and other applications, and are able to benefit from the control offered by a single material with several interconverted states. One example is reported by N. Branda,[205] where three dithienylethene (DTE) derivatives providing the three primary colors are covalently linked to norbonene-based water-soluble monomers. Thus, a new family of multiaddressable photoresponsive copolymers is prepared by ring-opening metathesis polymerization (ROMP). Since DTE compounds exhibit fast response times, good thermal stability of both isomers (colorless ring-open and colored ring-closed), high fatigue resistance and their structures can be easily modified, they are some of the most promising candidates for use in devices. For instance, a three-component hybrid system (CP4, **Figure 20**) has been successfully tested as multicolor barcode. Readers with interest on DTE-including materials and their application in memories, switches, and actuators can consult the review of M. Irie *et al.* [206]

Multicolor photochromism can also be provided by supramolecular coordination polymers accommodating guest water molecules and anions (perchlorates, halides, pseudo-halides…). [207] The soft metal organic hybrid material interacts with the environment, leading to a solvent- and anion-controlled photochromism via different charge transfers with the electron-accepting bipyridinium (viologen) moieties.

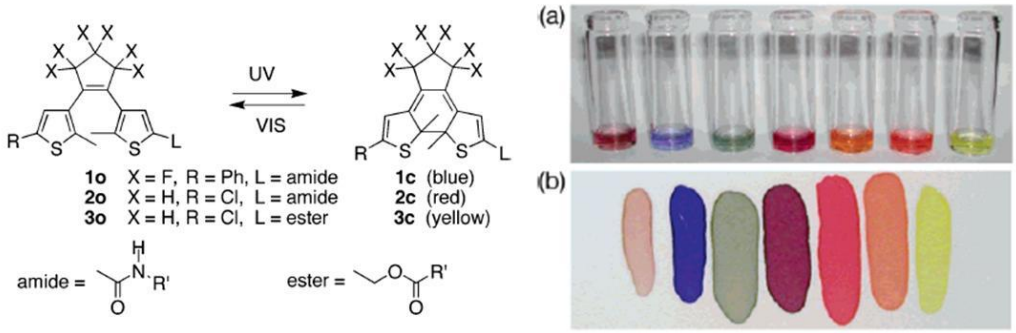

Figure 20. DTE derivatives whose ring-closed isomers exhibit primary colors. (a) Colors mixing of DTE homopolymers P1-P3 after THF solutions are irradiated with 313-nm light. The solutions contain (from left to right) [P1 + P2 + P3], [P1], [P1 + P3], [P1 + P2], [P2], [P2 + P3], and [P3]. (b) Samples of homo- and copolymers (from left to right) CP4, P1, CP2, CP1, P2, CP3, and P3 painted onto a silica plate followed by irradiation with 313-nm light. Adapted with permission from ref [205].

Multicolor systems combining photochromic dyes with grapheme have recently been published. S. Sharker developed a stimuli-responsive material based on graphene oxide coupled with a polymer conjugated with photochromic spiropyran dye and hydrophobic boron dipyrromethane dye, for application in triggered target multicolor bioimaging.[208] The different color of the functionalized graphene oxide is induced by both irradiation with UV light and by changing the pH from acidic to neutral. The stability, biocompatibility, and quenching efficacy of this nanocomposite open a different perspective for cell imaging in different independent colors, sequentially and simultaneously. Despite the efforts of the scientists on developing multicolor photochromic systems, most of them are based on polymers, [39] single crystals[207] or organogels[209, 210] containing organic moieties (no organic-inorganic hybrids), and they still present strong limitations for a real implementation in commercial devices.

3.3 Inorganic and organometallic photochromism in hybrids

The inorganic photochromism is mainly provided by silver nanoparticles, transition metal oxides such as WO_3, MoO_3 and Nb_2O_5, and polyoxometalates (POMs). The color changes are completely different to those of organic dyes, and the mechanisms usually involve the generation of electron-hole pairs and valence state variations in oxygen defect structures. Some composites and hybrid systems including inorganic photochromes have already been fabricated. Despite all the efforts of scientists, their use in technical applications such as erasable optical storage media, large-area displays, chemical sensors, control of radiation intensity or self-developing photography is still incipient due to the necessity of improving the variety of colors and the kinetics of coloration and fading.

A brief review of photochromic hybrids of metal halides, cyanides and chalcogenides, polyoxometalates, and metal–organic complexes was reported in 2010.[148] It is worth to note that there are references in the literature employing the term *hybrid* in the sense of composite material, and no organic moiety is included in the final compound. In most of the cases, organic molecules are employed in the synthetic procedure as structure-directing agents or templates. The readers will find below some of the major advances in inorganic and organometallic photochromism.

The photochromic activity of silver halides lays on its dissociation into colloidal silver upon UV radiation. Its use in ophthalmic lenses is well-known since the sixties, but the development of new materials with a wider palette of colors, faster bleaching kinetics, lower density, etc. is still a subject of extensive investigation. Numerous papers reporting smart photochromic properties of Ag[211-215] species deposited onto TiO_2 substrates have appeared in the last years. Interesting properties are developed in titanate nanotubes loaded with AgCl or Ag NPs.[216] For AgCl–titanate nanotubes (TNTs), the photochromic behavior consists on the red colouration on the material after irradiation by red light due to the photoreduction of silver halide to Ag nanoparticles. In the case of Ag NPs loaded TNTs, the materials exhibit multicolor photochromism corresponding to that of incident light associated to particle-plasmon-assisted electron transfer from Ag nanoparticles to TiO_2. This example reveals how important is to control the active species and the photochromic mechanism involved in the photo- and electro-optical processes.

One interesting advance in terms of industrial application is reported by F. Tricot[214] in 2015 who prepared a flexible Ag:TiO_2 photochromic material using ink-jet and flexography printing processes compatible with industrial scale production (**Figure 21**). For that, a titanium precursor solution is printed on a plastic substrate thanks to adaptation of printing processes. After incorporating silver, the coating shows a reversible photochromic behavior with a good contrast between the colored and bleached state. This breakthrough technology offers a new means to store updatable data and to secure products in smart cards or goods packaging areas.

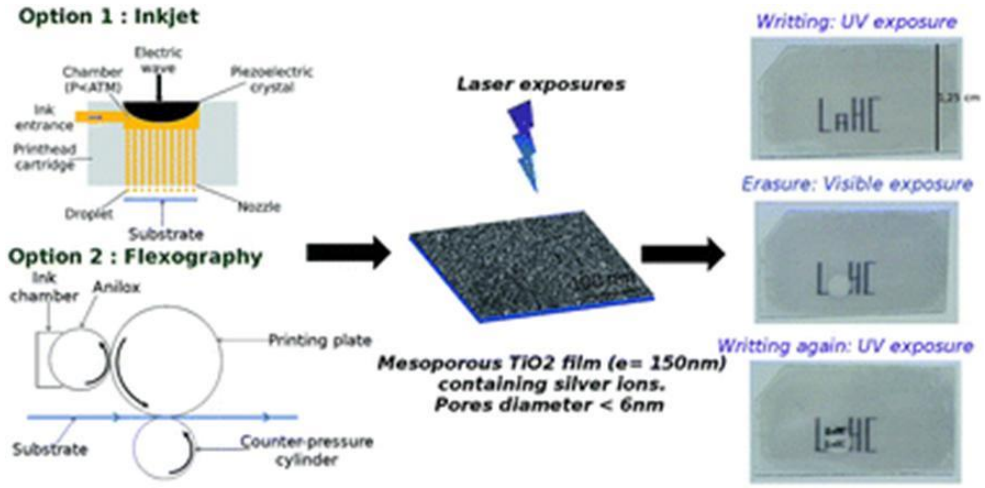

Figure 21. Principle of inkjet and flexography process (left), description of the Ag:TiO_2 material (center) and pictures of UV exposure inscription and visible exposure erasing on a film coated by flexography (right).

Cheaper Cu NPs exhibiting unique photochromic properties onto TiO_2 substrates have also appeared. The special feature is that copper can exhibit three oxidation states, Cu^{2+}, Cu^{+} and Cu^{0}. The redox process associated to photochromism can be controlled by varying the light source and exposure time. For instance, D. M. Tobaldi [217] reports Cu-TiO_2 hybrid nanoparticles with tunable photochromism under both UVA and visible-light exposure. The material is 2 nm Cu NPs decorating the surface of ~10 nm TiO_2 NPs. Under UVA, Cu^{2+} is completely reduced to Cu^{0} in few minutes (the d-d absorption band lowers to 95% after 10 min). Under visible-light, Cu^{2+} reduces only to Cu^{+} and in a lesser extent (80% in 1 h under visible-light). This rapid and sensitive effect can potentially be used to modify, tune, or monitor the progress of photoactivated behavior in a new generation of smart/active multifunctional materials and photoactive devices or sensors.

Regarding photochromic WO_3 and MoO_3 materials, significant advances have been made in the past decades, such as the response to visible light, and the improved photochromism by proton donors.[218, 219] However, organic-inorganic hybrid derivatives could solve other critical questions: (i) to improve reversibility; (ii) to fabricate systems exhibiting a wide variety of colors; and (iii) to enhance the sensitivity of the photochromic effect in the near-ultraviolet range. Some groups have investigated the intercalation of organic molecules such as diaminoalkane, phenethylamine, pyridine and poly(ethylene glycol) in the interlayer space of both structures, WO_3 and MoO_3. [220-223] A nice example is the preparation of tungsten oxide layers intercalated with acetic acid and hexamethylenetetramine (HMT) molecules with a 3D flowerlike morphology. [224] The most important result of the work is the good reversibility (as high as 98.4%, which is much higher than conventional WO_3 materials) and the good coloration response expanded to the visible-light region, which is a critical challenge for practical applications using solar energy and other visible laser sources. A second approach is to develop anisotropic organic–inorganic nano-hybrids,[225] in which the 1D organization of MoO_x nanoclusters enhances the photochromic sensitivity, and tunable components endow them with tailored performance.
Numerous studies have reported the preparation of photochromic WO_3 and MoO_3 shaped as thin films,[226-228] nanorods[229], nanowires[229] or nanoflakes[230] in the last decade, but very few are devoted to real organic-inorganic hybrids. In those reports, organic molecules (EDTA, [229] citric acid [231], etc.) are used to prevent the uncontrolled precipitation of the inorganic oxides and also act as directing agents, giving to tunable morphologies and photochromism.

Only one paper[232] that reports tungsten oxide included in a fluoro-polymer matrix yield a modest photochromic response. Only a 40% of transparency is obtained, so further improvements are necessary for a real application.

The photochromic properties of tungsten and molybdenum oxides can be modified by interaction with different inorganic species such as CdS NPs,[233] Ag[234]/Cu[227] species, TiO_2,[235, 236] silica,[237] or cellulose.[238] These nanocomposite materials are not strictly hybrid organic-inorganic materials, so these issues are out of the scope of this manuscript.

Photochromic polyoxometalates (POMs) are by far the most studied systems in the last years. A complete report about photochromism in composites and hybrid materials based on polyoxometalates was reported in 2006.[147] POMs can be organically-modified inorganic metal-oxygen cluster anions (i.e. polyoxomolybdates and polyoxotungstates), and they are promising candidates for photochromic applications due to their highly versatile and tunable structural, chemical, and redox properties. POMs, upon UV or VIS radiation, are able to accept electrons and/or protons from organic donor counter-cations in a reversibly exchange without decomposing or undergoing changes to its structural arrangement, to become mixed valence colored species (*heteropolyblues* or *heteropolybrowns*). In these complex structures, the organic moieties play an important role in the optical processes since purely inorganic POMs have no reversible photochromism and the colour change is not attractive. In general, the photo-generated colors of these hybrids depend upon the chemical composition and topology of the POMs, while the coloration and fading kinetics of these compounds are related to the nature of the organic cations and their interactions at the organic–inorganic interface. Therefore, much attention has been dedicated to the effective modification of photochromic properties using different organic moieties. Among them, we can cite an interesting work in which photochromic organic-inorganic materials are constructed via the coupling of liquid-crystalline nonionic surfactants and polyoxometalates (POMs).[239] The chemical interaction of the complex nanostructures with organic molecules from the environment (solvent, air, etc.) has a clear effect in the photochromic response, providing new sensors and smart catalysts. An interesting work has been reported in 2009,[240] metal-organic frameworks constructed from titanium-oxo clusters and dicarboxylate linkers, exhibit a reversible photochromic behavior induced by alcohol adsorption.

The combination of POMs with organic dyes to enhance the activity or to provide new multichromic hybrid organic–inorganic supramolecular assemblies has also been explored. For instance, spiropyran molecules, with high photochromic performance, have been recently integrated in POM structures via covalent bonds[241-243] and non-covalent interactions[244, 245] with different performances.

The systematic study of Hakouk et al. [242] is especially interesting since they analyze the photochromic behavior taking into account several physical parameters (SP structural characteristics, SP/POM and SP/solvent solid-state interactions, molar volume, etc). The study reveals that the coloration of the materials before UV exposure is governed by a low-energy intermolecular charge-transfer (CT) transition between SP donor and POM acceptor (see **Figure 22**). The CT transition energy can be tailored by tuning the intrinsic ligand-to-metal charge-transfer (LMCT) of the POM unit, which allows drastic improvement of the photocoloration contrasts.

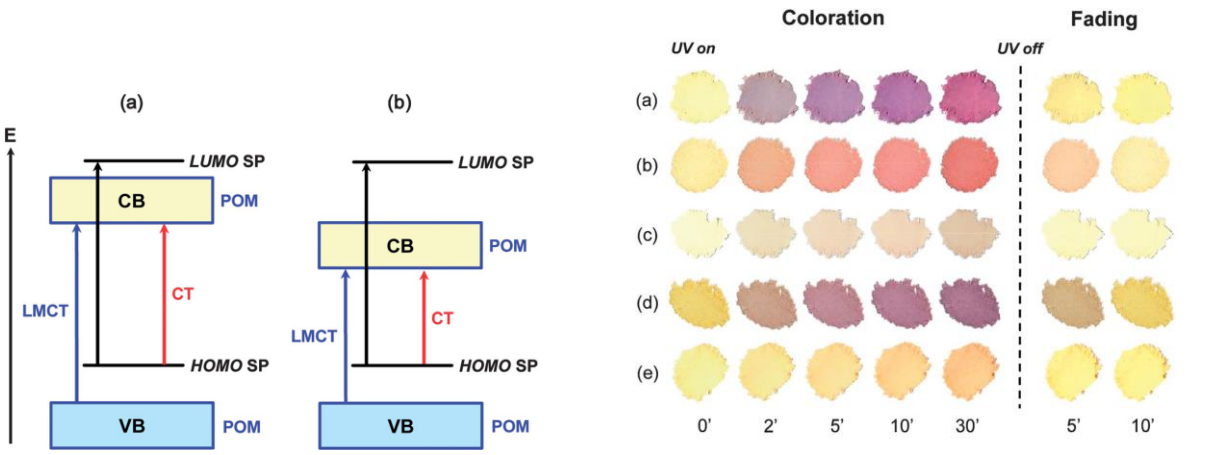

Figure 22. Schematic energetic diagrams displaying the three absorption phenomena predictable in SP-POM self-assembled structures when the SP cation is assembled with a POM unit having (a) a high-energy LMCT transition and (b) a low-energy LMCT transition. Photographs of powders of (a) $SP_4Mo_8.CH_3CN$, (b) $SP_4Mo_8.DMSO$, (c) $SP_4Mo_8.DMF$, (d) SP_3Mo_8, and (e) SP_2AlMo_6 at different time during the coloration process under UV irradiation (365 nm – 6 W), and the fading process under ambient light at room temperature.[242]

Furthermore, most of these systems exhibit electrochromism (**Figure 23**). Also cucurbituril-POMs dyads[246] exhibit reversible photochromic properties as well as excellent photocatalytic activities toward the degradation of methyl orange (MO) and rhodamine-B (RB) under visible light irradiation. Interconversion pathways and chemical factors affecting the stabilization of the different species are highlighted and discussed in hybrids based on DABCO[247], piperazine and molybdate. [248]
Some exotic systems such as 3D iodoplumbate open-framework material exhibited interesting wavelength-dependent photochromic properties.[249]

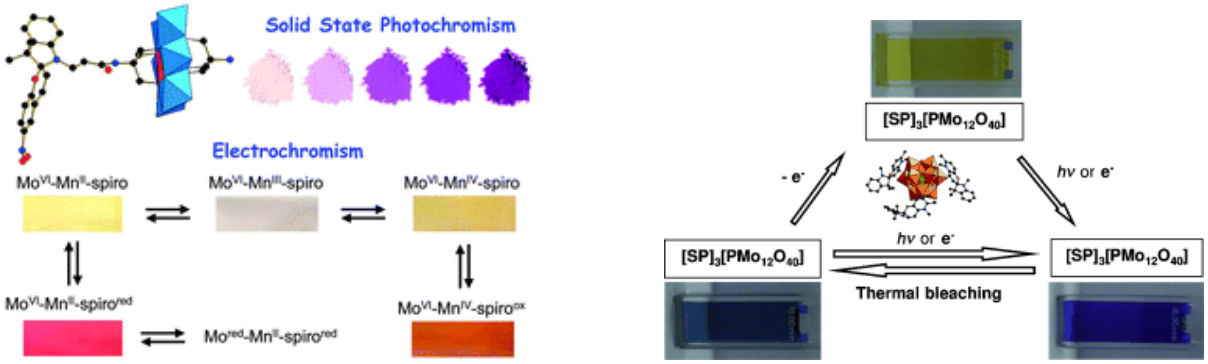

Figure 23. Structures of dual photochromic/electrochromic compounds based on spiropyrans and polyoxometalates with "covalent bonding" (left)[241] and "electrostatic interaction" (right).[244]

However, to apply them in useful devices, the challenge is to encapsulate or integrate POMs into organic, polymeric or inorganic matrices or substrates to find new materials with adequate optical, mechanical, and chemical properties and applications such as catalysis, energy storage or biomedicine.[250] The first attempt to process photoactive porous POMs as thin films with high optical quality have already been done.[251] The work presents a simple route for the preparation of colloids of a flexible porous iron carboxylate (MIL-89) with

tailored sorption properties that can be extended to other polyoxometallates and metal-organic frameworks.

Mesoporous bulk silicas have been used as supports for the immobilization of photochromic POMs by co-condensation and direct post-grafting, both based on covalent bonding and by impregnation[245, 252, 253] Photochromic POMs have also been introduced in bulk silica matrices by sol–gel to produce POM/silica hybrid films.[254, 255] Other works explore non-covalent interactions between the photochromic species and the matrix, such as the lanthano phosphomolybdates anions immobilized through electrostatic forces onto positively-charged silica nanoparticles.[256] Ormosils like tri-ureasils have also been used to embed POMs providing transparent, flexible and rubbery photochromic materials.[245, 257]

References

[1] J. R. Lakowicz, *Principles of Fluorescence Spectroscopy*, Springer US, New York 2006.
[2] B. Valeur, M. N. Berberan-Santos, *Molecular Fluorescence: Principles and Applications*, John Wiley & Sons, Weinheim 2012.
[3] N. J. Turro, *Modern Molecular Photochemistry*, University Science Books, Sausalito, CA 1991.
[4] A. Kohler, J. S. Wilson, R. H. Friend, *Adv. Mater.* **2002**, *14*, 701.
[5] K. K. Ng, G. Zheng, *Chem. Rev.* **2015**, *115*, 11012.
[6] J. Z. Zhao, S. M. Ji, H. M. Guo, *RSC Adv.* **2011**, *1*, 937.
[7] G. Blasse, B. C. Grabmaier, *Luminescent Materials*, Springer-Verlag, Berlin 1994.
[8] D. B. Mitzi, K. Chondroudis, C. R. Kagan, *IBM J. Res. Dev.* **2001**, *45*, 29.
[9] E. R. Dohner, E. T. Hoke, H. I. Karunadasa, *J. Am. Chem. Soc.* **2014**, *136*, 1718.
[10] Y. H. Kim, H. Cho, J. H. Heo, T. S. Kim, N. Myoung, C. L. Lee, S. H. Im, T. W. Lee, *Adv. Mater.* **2015**, *27*, 1248.
[11] T. Dantas de Morais, F. Chaput, J. P. Boilot, K. Lahlil, B. Darracq, Y. Levy, *C.R. Acad. Sci. IV-Phys.* **2000**, *1*, 479.
[12] O. J. Dautel, G. Wantz, R. Almairac, D. Flot, L. Hirsch, J. P. Lere-Porte, J. P. Parneix, F. Serein-Spirau, L. Vignau, J. J. E. Moreau, *J. Am. Chem. Soc.* **2006**, *128*, 4892.
[13] N. Mizoshita, Y. Goto, Y. Maegawa, T. Tani, S. Inagaki, *Chem. Mater.* **2010**, *22*, 2548.
[14] X. H. Yang, T. Giovenzana, B. Feild, G. E. Jabbour, A. Sellinger, *J. Mater. Chem.* **2012**, *22*, 12689.
[15] H. S. Jung, Y. J. Kim, S. W. Ha, J. K. Lee, *J. Mater. Chem. C* **2013**, *1*, 5879.
[16] Y. Kajiwara, A. Nagai, K. Tanaka, Y. Chujo, *J. Mater. Chem. C* **2013**, *1*, 4437.
[17] S. Y. Kwak, S. Yang, N. R. Kim, J. H. Kim, B. S. Bae, *Adv. Mater.* **2011**, *23*, 5767.
[18] E. Carregal-Romero, A. Llobera, V. J. Cadarso, M. Darder, P. Aranda, C. Dominguez, E. Ruiz-Hitzky, C. Fernandez-Sanchez, *ACS Appl. Mater. Interfaces* **2012**, *4*, 5029.
[19] Y. Yuan, M. Kruger, *Polymers-Basel* **2012**, *4*, 1.
[20] J. D. Furman, A. Y. Warner, S. J. Teat, A. A. Mikhailovsky, A. K. Cheetham, *Chem. Mater.* **2010**, *22*, 2255.
[21] A. Kojima, K. Teshima, Y. Shirai, T. Miyasaka, *J. Am. Chem. Soc.* **2009**, *131*, 6050.
[22] W. S. Yang, J. H. Noh, N. J. Jeon, Y. C. Kim, S. Ryu, J. Seo, S. I. Seok, *Science* **2015**, *348*, 1234.
[23] Y. X. Zhao, K. Zhu, *Chem. Soc. Rev.* **2016**, *45*, 655.
[24] R. Houbertz, G. Domann, C. Cronauer, A. Schmitt, H. Martin, J. U. Park, L. Frohlich, R. Buestrich, M. Popall, U. Streppel, P. Dannberg, C. Wachter, A. Brauer, *Thin Solid Films* **2003**, *442*, 194.
[25] L. D. Carlos, R. A. S. Ferreira, V. de Zea Bermudez, S. J. L. Ribeiro, *Adv. Mater.* **2009**, *21*, 509.
[26] R. A. S. Ferreira, P. S. Andre, L. D. Carlos, *Opt. Mater.* **2010**, *32*, 1397.
[27] C. Sanchez, P. Belleville, M. Popall, L. Nicole, *Chem. Soc. Rev.* **2011**, *40*, 696.
[28] L. D. Carlos, R. A. S. Ferreira, V. de Zea Bermudez, B. Julián-López, P. Escribano, *Chem. Soc. Rev.* **2011**, *40*, 536.
[29] B. Lebeau, P. Innocenzi, *Chem. Soc. Rev.* **2011**, *40*, 886.
[30] M. Zayat, R. Pardo, E. Castellón, L. Torres, D. Almendro, P. G. Parejo, A. Álvarez, T. Belenguer, S. García-Revilla, R. Balda, J. Fernández, D. Levy, *Adv. Mater.* **2011**, *23*, 5318.
[31] C. Sanchez, F. Ribot, *New J. Chem.* **1994**, *18*, 1007.
[32] R. Reisfeld, D. Shamrakov, C. Jorgensen, *Sol. Energy Mater. Sol. Cells* **1994**, *33*, 417.

[33] Y. Yang, M. Q. Wang, G. D. Qian, Z. Y. Wang, X. P. Fan, *Opt. Mater.* **2004**, *24*, 621.
[34] B. Lebeau, N. Herlet, J. Livage, C. Sanchez, *Chem. Phys. Lett.* **1993**, *206*, 15.
[35] T. H. Nhung, M. Canva, F. Chaput, H. Goudket, G. Roger, A. Brun, D. D. Manh, N. D. Hung, J. P. Boilot, *Opt. Commun.* **2004**, *232*, 343.
[36] B. Julián-López, R. Corberan, E. Cordoncillo, P. Escribano, B. Viana, C. Sanchez, *J. Mater. Chem.* **2004**, *14*, 3337.
[37] E. Pecoraro, S. García-Revilla, R. A. S. Ferreira, R. Balda, L. D. Carlos, J. Fernandez, *Opt. Express* **2010**, *18*, 7470.
[38] Y. Kajiwara, A. Nagai, Y. Chujo, *J. Mater. Chem.* **2010**, *20*, 2985.
[39] X. Zhang, W. Liu, G. Z. Wei, D. Banerjee, Z. C. Hu, J. Li, *J. Am. Chem. Soc.* **2014**, *136*, 14230.
[40] S. Dire, F. Babonneau, C. Sanchez, J. Livage, *J. Mater. Chem.* **1992**, *2*, 239.
[41] R. de Francisco, M. Hoyos, N. Garcia, P. Tiemblo, *Langmuir* **2015**, *31*, 3718.
[42] I. Roppolo, M. Messori, S. Perruchas, T. Gacoin, J. P. Boilot, M. Sangermano, *Macromol. Mater. Eng.* **2012**, *297*, 680.
[43] B. Viana, N. Koslova, P. Aschehoug, C. Sanchez, *J. Mater. Chem.* **1995**, *5*, 719.
[44] N. Pradal, D. Boyer, G. Chadeyron, S. Therias, A. Chapel, C. V. Santilli, R. Mahiou, *J. Mater. Chem. C* **2014**, *2*, 6301.
[45] A. Potdevin, G. Chadeyron, S. Therias, R. Mahiou, *Langmuir* **2012**, *28*, 13526.
[46] C. Sanchez, B. Lebeau, F. Chaput, J. P. Boilot, *Adv. Mater.* **2003**, *15*, 1969.
[47] C. Sanchez, B. Julian, P. Belleville, M. Popall, *J. Mater. Chem.* **2005**, *15*, 3559.
[48] L. Nicole, L. Rozes, C. Sanchez, *Adv. Mater.* **2010**, *22*, 3208.
[49] P. Escribano, B. Julián-López, J. Planelles-Aragó, E. Cordoncillo, B. Viana, C. Sanchez, *J. Mater. Chem.* **2008**, *18*, 23.
[50] K. Binnemans, *Chem. Rev.* **2009**, *109*, 4283.
[51] J. Feng, H. Zhang, *Chem. Soc. Rev.* **2013**, *42*, 387.
[52] S. J. L. Ribeiro, M. V. dos Santos, R. R. Silva, E. Pecoraro, R. R. Gonçalves, J. M. A. Caiut, in *The Sol-Gel Handbook*, Vol. 3 (Eds: D. Levy, M. Zayat), Wiley-VCH Verlag GmbH & Co. KGaA, Weinheim 2015, 929.
[53] V. T. Freitas, R. A. S. Ferreira, L. D. Carlos, in *The Sol-Gel Handbook*, Vol. 3 (Eds: D. Levy, M. Zayat), Wiley-VCH Verlag GmbH & Co. KGaA, Weinheim 2015, 883.
[54] G. Y. Chen, H. L. Qju, P. N. Prasad, X. Y. Chen, *Chem. Rev.* **2014**, *114*, 5161.
[55] G. Y. Chen, I. Roy, C. H. Yang, P. N. Prasad, *Chem. Rev.* **2016**, *116*, 2826.
[56] M. Montalti, L. Prodi, E. Rampazzo, N. Zaccheroni, *Chem. Soc. Rev.* **2014**, *43*, 4243.
[57] J. C. G. Bunzli, *J. Lumin.* **2016**, *170*, 866.
[58] C. W. Tang, S. A. Vanslyke, *Appl. Phys. Lett.* **1987**, *51*, 913.
[59] R. Reisfeld, D. Brusilovsky, M. Eyal, E. Miron, Z. Burstein, J. Ivri, *Chem. Phys. Lett.* **1989**, *160*, 43.
[60] J. C. Altman, R. E. Stone, B. Dunn, F. Nishida, *IEEE Photonic. Tech. Lett.* **1991**, *3*, 189.
[61] X. X. He, J. H. Duan, K. M. Wang, W. H. Tan, X. Lin, C. M. He, *J. Nanosci. Nanotechno.* **2004**, *4*, 585.
[62] T. Dantas de Morais, F. Chaput, K. Lahlil, J. P. Boilot, *Adv. Mater.* **1999**, *11*, 107.
[63] F. Olivero, F. Carniato, C. Bisio, L. Marchese, *J. Mater. Chem.* **2012**, *22*, 25254.
[64] S. L. Burkett, A. Press, S. Mann, *Chem. Mater.* **1997**, *9*, 1071.
[65] A. J. Patil, S. Mann, *J. Mater. Chem.* **2008**, *18*, 4605.
[66] K. V. Rao, K. K. R. Datta, M. Eswaramoorthy, S. J. George, *Adv. Mater.* **2013**, *25*, 1713.
[67] K. V. Rao, A. Jain, S. J. George, *J. Mater. Chem. C* **2014**, *2*, 3055.
[68] A. Jain, A. Achari, M. Eswaramoorthy, S. J. George, *J. Mater. Chem. C* **2016**, *4*, 2748.

[69] C. Y. Huang, Y. K. Su, T. C. Wen, T. F. Guo, M. L. Tu, *IEEE Photonic Tech. Lett.* **2008**, *20*, 282.
[70] C. Y. Huang, T. S. Huang, C. Y. Cheng, Y. C. Chen, C. T. Wan, M. V. M. Rao, Y. K. Su, *IEEE Photonic Tech. Lett.* **2010**, *22*, 305.
[71] H. Y. Lin, S. W. Wang, C. C. Lin, K. J. Chen, H. V. Han, Z. Y. Tu, H. H. Tu, T. M. Chen, M. H. Shih, P. T. Lee, H. M. P. Chen, H. C. Kuo, *IEEE J. Sel. Top. Quant. Electron.* **2016**, *22*.
[72] J. Chen, W. Liu, L.-H. Mao, Y.-J. Yin, C.-F. Wang, S. Chen, *J. Mater. Sci.* **2014**, *49*, 7391.
[73] X. Bai, G. Caputo, Z. D. Hao, V. T. Freitas, J. H. Zhang, R. L. Longo, O. L. Malta, R. A. S. Ferreira, N. Pinna, *Nat. Commun.* **2014**, *5*.
[74] K. Lee, K. Cheah, B. An, M. Gong, Y. L. Liu, *Appl. Phys. A* **2005**, *80*, 337.
[75] X. G. Huang, G. Zucchi, J. Tran, R. B. Pansu, A. Brosseau, B. Geffroy, F. Nief, *New J. Chem.* **2014**, *38*, 5793.
[76] Y. Lu, B. Yan, *Chem. Commun.* **2014**, *50*, 15443.
[77] H. G. Yan, H. H. Wang, P. He, J. X. Shi, M. L. Gong, *Synthetic Met.* **2011**, *161*, 748.
[78] S. García-Revilla, J. Fernandez, M. A. Illarramendi, B. García-Ramiro, R. Balda, H. Cui, M. Zayat, D. Levy, *Opt. Express* **2008**, *16*, 12251.
[79] D. S. Wiersma, *Nat. Phys.* **2008**, *4*, 359.
[80] S. García-Revilla, J. Fernandez, M. Barredo-Zuriarrain, L. D. Carlos, E. Pecoraro, I. Iparraguirre, J. Azkargorta, R. Balda, *Opt. Express* **2015**, *23*, 1456.
[81] B. Redding, M. A. Choma, H. Cao, *Opt. Lett.* **2011**, *36*, 3404.
[82] B. Redding, M. A. Choma, H. Cao, *Nat. Photonics* **2012**, *6*, 355.
[83] E. P. Giannelis, A. Stasinopoulos, M. Psyllaki, G. Zacharakis, R. N. Das, D. Anglos, S. H. Anastasiadis, R. A. Vaia, *Mater. Res. Soc. Symp. Proc.* **2002**, *726*, 11.
[84] D. Anglos, A. Stassinopoulos, R. N. Das, G. Zacharakis, M. Psyllaki, R. Jakubiak, R. A. Vaia, E. P. Giannelis, S. H. Anastasiadis, *J. Opt. Soc. Am. B* **2004**, *21*, 208.
[85] S. García-Revilla, M. Zayat, R. Balda, M. Al-Saleh, D. Levy, J. Fernandez, *Opt. Express* **2009**, *17*, 13202.
[86] X. G. Meng, K. Fujita, Y. H. Zong, S. Murai, K. Tanaka, *Appl. Phys. Lett.* **2008**, *92*.
[87] L. Cerdan, A. Costela, I. Garcia-Moreno, *Org. Electron.* **2012**, *13*, 1463.
[88] A. Costela, I. Garcia-Moreno, L. Cerdan, V. Martin, O. Garcia, R. Sastre, *Adv. Mater.* **2009**, *21*, 4163.
[89] P. Gorrn, M. Lehnhardt, W. Kowalsky, T. Riedl, S. Wagner, *Adv. Mater.* **2011**, *23*, 869.
[90] O. V. Sakhno, J. Stumpe, T. N. Smirnova, *Appl. Phys. B-Lasers O* **2011**, *103*, 907.
[91] R. R. da Silva, C. T. Dominguez, M. V. dos Santos, R. Barbosa-Silva, M. Cavicchioli, L. M. Christovan, L. S. A. de Melo, A. S. L. Gomes, C. B. de Araujo, S. J. L. Ribeiro, *J. Mater. Chem. C* **2013**, *1*, 7181.
[92] D. C. Oliveira, Y. Messaddeq, K. Dahmouche, S. J. L. Ribeiro, R. R. Goncalves, A. Vesperini, D. Gindre, J. M. Nunzi, *J. Sol-Gel Sci. Technol.* **2006**, *40*, 359.
[93] R. Reisfeld, S. Neuman, *Nature* **1978**, *274*, 144.
[94] R. Reisfeld, Y. Kalisky, *Nature* **1980**, *283*, 281.
[95] B. M. van der Ende, L. Aarts, A. Meijerink, *Phys. Chem. Chem. Phys.* **2009**, *11*, 11081.
[96] N. C. Giebink, G. P. Wiederrecht, M. R. Wasielewski, *Nat. Photonics* **2011**, *5*, 695.
[97] X. Huang, S. Han, W. Huang, X. Liu, *Chem. Soc. Rev.* **2013**, *42*, 173.
[98] C. H. Chou, J. K. Chuang, F. C. Chen, *Sci. Rep.* **2013**, *3*, 2244.
[99] J.-C. G. Bünzli, A.-S. Chauvin, in *Handbook on the Physics and Chemistry of Rare-Earths*, Vol. 44 (Eds: J.-C. G. Bünzli, V. K. Pecharsky), Elsevier B. V., Amsterdam 2014, 169.

[100] S. F. H. Correia, V. de Zea Bermudez, S. J. L. Ribeiro, P. S. André, R. A. S. Ferreira, L. D. Carlos, *J. Mater. Chem. A* **2014**, *2*, 5580.
[101] S. F. H. Correia, P. P. Lima, L. D. Carlos, P. S. André, R. A. S. Ferreira, *Prog. Photovolt: Res. Appl.* **2016**, 10.1002/pip.2772.
[102] B. C. Rowan, L. R. Wilson, B. S. Richards, *IEEE J. Sel. Top. Quant.* **2008**, *14*, 1312.
[103] R. Reisfeld, C. K. Jorgensen, *Struct. Bond.* **1982**, *49*, 1.
[104] R. Reisfeld, *Opt. Mater.* **2010**, *32*, 850.
[105] F. Meinardi, A. Colombo, K. A. Velizhanin, R. Simonutti, M. Lorenzon, L. Beverina, R. Viswanatha, V. I. Klimov, S. Brovelli, *Nat. Photonics* **2014**, *8*, 392.
[106] F. Meinardi, H. McDaniel, F. Carulli, A. Colombo, K. A. Velizhanin, N. S. Makarov, R. Simonutti, V. I. Klimov, S. Brovellii, *Nat. Nanotechnol.* **2015**, *10*, 878.
[107] Y. Zhao, R. R. Lunt, *Adv. Energy Mater.* **2013**, *3*, 1143.
[108] J. Graffion, X. Cattoën, M. Wong Chi Man, V. R. Fernandes, P. S. André, R. A. S. Ferreira, L. D. Carlos, *Chem. Mater.* **2011**, *23*, 4773.
[109] J. Graffion, A. M. Cojocariu, X. Cattoën, R. A. S. Ferreira, V. R. Fernandes, P. S. André, L. D. Carlos, M. Wong Chi Man, J. R. Bartlett, *J. Mater. Chem.* **2012**, *22*, 13279.
[110] V. T. Freitas, L. S. Fu, A. M. Cojocariu, X. Cattoën, J. R. Bartlett, R. Le Parc, J. L. Bantignies, M. Wong Chi Man, P. S. André, R. A. S. Ferreira, L. D. Carlos, *ACS Appl. Mater. Interfaces* **2015**, *7*, 8770.
[111] M. M. Nolasco, P. M. Vaz, V. T. Freitas, P. P. Lima, P. S. André, R. A. S. Ferreira, P. D. Vaz, P. Ribeiro-Claro, L. D. Carlos, *J. Mater. Chem. A* **2013**, *1*, 7339.
[112] S. F. H. Correia, P. P. Lima, P. S. André, R. A. S. Ferreira, L. D. Carlos, *Sol. Energy Mater. Sol. Cells* **2015**, *138*, 51.
[113] A. Kaniyoor, B. McKenna, S. Comby, R. C. Evans, *Adv. Opt. Mater.* **2016**, *4*, 444.
[114] W. Wu, T. Wang, X. Wang, S. Wu, Y. Luo, X. Tian, Q. Zhang, *Sol. Energy* **2010**, *84*, 2140.
[115] R. H. Inman, G. V. Shcherbatyuk, D. Medvedko, A. Gopinathan, S. Ghosh, *Opt. Express* **2011**, *19*, 24308.
[116] E. H. Banaei, A. F. Abouraddy, *Proc. SPIE* **2013**, *8821*, 882102.
[117] K. R. McIntosh, N. Yamada, B. S. Richards, *Appl. Phys. B* **2007**, *88*, 285.
[118] A. Millán, L. D. Carlos, C. D. S. Brites, N. J. O. Silva, R. Piñol, F. Palacio, in *Thermometry at the nanoscale: Techniques and selected applications*, (Eds: L. D. Carlos, F. Palacio), Royal Society of Chemistry, Oxfordshire 2016, 237.
[119] C. D. S. Brites, P. P. Lima, N. J. O. Silva, A. Millán, V. S. Amaral, F. Palacio, L. D. Carlos, *Adv. Mater.* **2010**, *22*, 4499.
[120] W. Jung, Y. W. Kim, D. Yim, J. Y. Yoo, *Sensor Actuat. A-Phys.* **2011**, *171*, 228.
[121] D. Wawrzynczyk, A. Bednarkiewicz, M. Nyk, W. Strek, M. Samoc, *Nanoscale* **2012**, *4*, 6959.
[122] L. M. Maestro, E. M. Rodriguez, F. S. Rodriguez, M. C. I. la Cruz, A. Juarranz, R. Naccache, F. Vetrone, D. Jaque, J. A. Capobianco, J. G. Sole, *Nano Lett.* **2010**, *10*, 5109.
[123] K. Okabe, N. Inada, C. Gota, Y. Harada, T. Funatsu, S. Uchiyama, *Nat. Commun.* **2012**, *3*, 705.
[124] O. A. Savchuk, P. Haro-Gonzalez, J. J. Carvajal, D. Jaque, J. Massons, M. Aguilo, F. Diaz, *Nanoscale* **2014**, *6*, 9727.
[125] A. H. Khalid, K. Kontis, *Meas. Sci. Technol.* **2009**, *20*, 025305.
[126] V. Lojpur, Z. Antic, M. D. Dramicanin, *Phys. Chem. Chem. Phys.* **2014**, *16*, 25636.
[127] C. D. S. Brites, P. P. Lima, N. J. O. Silva, A. Millán, V. S. Amaral, F. Palacio, L. D. Carlos, *Nanoscale* **2012**, *4*, 4799.
[128] D. Jaque, F. Vetrone, *Nanoscale* **2012**, *4*, 4301.
[129] X. D. Wang, O. S. Wolfbeis, R. J. Meier, *Chem. Soc. Rev.* **2013**, *42*, 7834.

[130] H. Y. Zhou, M. Sharma, O. Berezin, D. Zuckerman, M. Y. Berezin, *Chem. Phys. Chem.* **2016**, *17*, 27.
[131] L. D. Carlos, F. Palacio, *Thermometry at the nanoscale: Techniques and selected applications*, Royal Society of Chemistry, Oxfordshire 2016.
[132] J. M. Lupton, *Appl. Phys. Lett.* **2002**, *81*, 2478.
[133] D. P. Yan, J. Lu, J. Ma, M. Wei, D. G. Evans, X. Duan, *Angew. Chem. Int. Ed.* **2011**, *50*, 720.
[134] Z. P. Wang, D. Ananias, A. Carne-Sanchez, C. D. S. Brites, I. Imaz, D. Maspoch, J. Rocha, L. D. Carlos, *Adv. Funct. Mater.* **2015**, *25*, 2824.
[135] J. Lee, A. O. Govorov, N. A. Kotov, *Angew. Chem. Int. Ed.* **2005**, *44*, 7439.
[136] J. Li, X. Hong, Y. Liu, D. Li, Y. W. Wang, J. H. Li, Y. B. Bai, T. J. Li, *Adv. Mater.* **2005**, *17*, 163.
[137] R. Piñol, C. D. Brites, R. Bustamante, A. Martínez, N. J. Silva, J. L. Murillo, R. Cases, J. Carrey, C. Estepa, C. Sosa, F. Palacio, L. D. Carlos, A. Millán, *ACS Nano* **2015**, *9*, 3134.
[138] C. D. S. Brites, P. P. Lima, N. J. O. Silva, A. Millán, V. S. Amaral, F. Palacio, L. D. Carlos, *Front.Chem.* **2013**, *1*, 9.
[139] C. D. S. Brites, P. P. Lima, N. J. O. Silva, A. Millán, V. S. Amaral, F. Palacio, L. D. Carlos, *J. Lumin.* **2013**, *133*, 230.
[140] R. A. S. Ferreira, C. D. S. Brites, C. M. S. Vicente, P. P. Lima, A. R. N. Bastos, P. G. Marques, M. Hiltunen, L. D. Carlos, P. S. André, *Laser Photonics Rev.* **2013**, *7*, 1027.
[141] M. Rodrigues, R. Piñol, G. Antorrena, C. D. S. Brites, N. J. O. Silva, J. L. Murillo, R. Cases, I. Díez, F. Palacio, N. Torras, J. A. Plaza, L. Pérez-García, L. D. Carlos, A. Millán, *Adv. Funct. Mater.* **2016**, *26*, 200.
[142] H. Bouas-Laurent, H. Durr, *Pure Appl. Chem.* **2001**, *73*, 639.
[143] J. C. Crano, R. J. Guglielmetti, Eds., *Organic Photochromic and thermochromic compounds - Volume 1*, Vol. 1, Plenum Press, New York 1999.
[144] J. C. Crano, R. J. Guglielmetti, Eds., *Organic Photochromic and thermochromic compounds - Volume 2*, Vol. 2, Plenum Press, New York 1999.
[145] H. Dürr, H. Bouas-Laurent, Eds., *Photochromism: Molecules and Systems*, Elsevier, Amsterdam 2003.
[146] P. Bamfield, M. G. Hutchings, Eds., *Chromic Phenomena: Technological Applications of Colour Chemistry*, RSC Publishing, Cambridge 2010.
[147] T. He, J. Yao, *Prog. Mater. Sci.* **2006**, *51*, 810.
[148] M.-S. Wang, G. Xu, Z.-J. Zhang, G.-C. Guo, *Chem. Commun.* **2010**, *46*, 361.
[149] D. Levy, *Chem. Mater.* **1997**, *9*, 2666.
[150] R. Pardo, M. Zayat, D. Levy, *Chem. Soc. Rev.* **2011**, *40*, 672.
[151] D. Avnir, D. Levy, R. Reisfeld, *J. Phys. Chem.* **1984**, *88*, 5956.
[152] H. Behar-Levy, D. Avnir, *Chem. Mater.* **2002**, *14*, 1736.
[153] D. Levy, D. Avnir, *J. Photochem. Photobiol. A* **1991**, *57*, 41.
[154] D. Levy, S. Einhorn, D. Avnir, *J. Non-Cryst. Solids* **1989**, *113*, 137.
[155] F. Bentivegna, M. Canva, A. Brun, F. Chaput, J. P. Boilot, *J. Appl. Phys.* **1996**, *80*, 4655.
[156] F. Bentivegna, M. Canva, A. Brun, F. Chaput, J. P. Boilot, *J. Sol-Gel Sci. Technol.* **1997**, *9*, 33.
[157] F. Bentivegna, M. Canva, P. Georges, A. Brun, F. Chaput, L. Malier, J. P. Boilot, *Appl. Phys. Lett.* **1993**, *62*, 1721.
[158] J. P. Boilot, J. Biteau, F. Chaput, T. Gacoin, A. Brun, B. Darracq, P. Georges, Y. Levy, *Pure Appl. Opt.* **1998**, *7*, 169.
[159] M. Canva, G. Roger, F. Cassagne, Y. Levy, A. Brun, F. Chaput, J. P. Boilot, A. Rapaport, C. Heerdt, M. Bass, *Opt. Mater.* **2002**, *18*, 391.

[160] A. Dubois, M. Canva, A. Brun, F. Chaput, J. P. Boilot, *Synth. Met.* **1996**, *81*, 305.
[161] A. Dubois, M. Canva, A. Brun, F. Chaput, J. P. Boilot, *Appl. Opt.* **1996**, *35*, 3193.
[162] T. Fournier, T. H. Tranthi, N. Herlet, C. Sanchez, *Chem. Phys. Lett.* **1993**, *208*, 101.
[163] B. Lebeau, S. Brasselet, J. Zyss, C. Sanchez, *Chem. Mater.* **1997**, *9*, 1012.
[164] B. Lebeau, J. Maquet, C. Sanchez, E. Toussaere, R. Hierle, J. Zyss, *J. Mater. Chem.* **1994**, *4*, 1855.
[165] B. Lebeau, C. Sanchez, S. Brasselet, J. Zyss, G. Froc, M. Dumont, *New J. Chem.* **1996**, *20*, 13.
[166] B. Schaudel, C. Guermeur, C. Sanchez, K. Nakatani, J. A. Delaire, *J. Mater. Chem.* **1997**, *7*, 61.
[167] A. Lafuma, S. Chodorowski-Kimmes, F. X. Quinn, C. Sanchez, *Eur. J. Inorg. Chem.* **2003**, 331.
[168] M. Morimoto, S. Kobatake, M. Irie, *Photochem. Photobiol. Sci.* **2003**, *2*, 1088.
[169] M. Morimoto, S. Kobatake, M. Irie, *J. Am. Chem. Soc.* **2003**, *125*, 11080.
[170] M. Irie, T. Lifka, S. Kobatake, N. Kato, *J. Am. Chem. Soc.* **2000**, *122*, 4871.
[171] K. Amimoto, T. Kawato, *J. Photochem. Photobiol. C-Photochem. Rev.* **2005**, *6*, 207.
[172] J. Folling, S. Polyakova, V. Belov, A. van Blaaderen, M. L. Bossi, S. W. Hell, *Small* **2008**, *4*, 134.
[173] K. Kinashi, Y. Harada, Y. Ueda, *Thin Solid Films* **2008**, *516*, 2532.
[174] A. Bucko, S. Zielinska, E. Ortyl, M. Larkowska, R. Barille, *Opt. Mater.* **2014**, *38*, 179.
[175] T. Okada, M. Sohmiya, M. Ogawa, in *Photofunctional Layered Materials*, Vol. 166 (Eds: D. Yan, M. Wei), Springer Int Publishing Ag, Cham 2015, 177.
[176] G. Wirnsberger, B. J. Scott, B. F. Chmelka, G. D. Stucky, *Adv. Mater.* **2000**, *12*, 1450.
[177] A. Yamano, H. Kozuka, *Thin Solid Films* **2011**, *519*, 1772.
[178] F. Ribot, A. Lafuma, C. Eychenne-Baron, C. Sanchez, *Adv. Mater.* **2002**, *14*, 1496.
[179] R. A. Evans, T. L. Hanley, M. A. Skidmore, T. P. Davis, G. K. Such, L. H. Yee, G. E. Ball, D. A. Lewis, *Nat. Mater.* **2005**, *4*, 249.
[180] G. Such, R. A. Evans, L. H. Yee, T. P. Davis, *J. Macromol. Sci. Polymer Rev.* **2003**, *C43*, 547.
[181] P. J. Coelho, C. J. R. Silva, C. Sousa, S. D. F. C. Moreira, *J. Mater. Chem. C* **2013**, *1*, 5387.
[182] N. Mercier, *Eur. J. Inorg. Chem.* **2013**, 19.
[183] N. Leblanc, N. Mercier, M. Allain, O. Toma, P. Auban-Senzier, C. Pasquier, *J. Solid State Chem.* **2012**, *195*, 140.
[184] P.-X. Li, M.-S. Wang, M.-J. Zhang, C.-S. Lin, L.-Z. Cai, S.-P. Guo, G.-C. Guo, *Angew. Chem. Int. Ed.* **2014**, *53*, 11529.
[185] B. J. Coe, *Acc. Chem. Res.* **2006**, *39*, 383.
[186] M. Schulze, M. Utecht, A. Hebert, K. Rueck-Braun, P. Saalfrank, P. Tegeder, *J. Phys. Chem. Lett.* **2015**, *6*, 505.
[187] S. Gago, I. M. Fonseca, A. J. Parola, *Microporous Mesoporous Mater.* **2013**, *180*, 40.
[188] Y. Wu, X. Z. Qu, L. Y. Huang, D. Qiu, C. L. Zhang, Z. P. Liu, Z. Z. Yang, L. Feng, *J. Colloid Interface Sci.* **2010**, *343*, 155.
[189] J. Allouche, A. Le Beulze, J.-C. Dupin, J.-B. Ledeuil, S. Blanc, D. Gonbeau, *J. Mater. Chem.* **2010**, *20*, 9370.
[190] N. Vazquez-Mera, C. Roscini, J. Hernando, D. Ruiz-Molina, *Adv. Opt. Mater.* **2013**, *1*, 631.
[191] N. Andersson, P. Alberius, J. Ortegren, M. Lindgren, L. Bergstrom, *J. Mater. Chem.* **2005**, *15*, 3507.
[192] L. A. Connal, G. V. Franks, G. G. Qiao, *Langmuir* **2010**, *26*, 10397.
[193] S. A. Díaz, L. Giordano, T. M. Jovin, E. A. Jares-Erijman, *Nano Lett.* **2012**, *12*, 3537.

[194] C.-J. Carling, J.-C. Boyer, N. R. Branda, *J. Am. Chem. Soc.* **2009**, *131*, 10838.
[195] J.-C. Boyer, C.-J. Carling, B. D. Gates, N. R. Branda, *J. Am. Chem. Soc.* **2010**, *132*, 15766.
[196] C.-J. Carling, J.-C. Boyer, N. R. Branda, *Org. Biomol. Chem.* **2012**, *10*, 6159.
[197] R. Klajn, J. F. Stoddart, B. A. Grzybowski, *Chem. Soc. Rev.* **2010**, *39*, 2203.
[198] H. Nishi, T. Asahi, S. Kobatake, *J. Phys. Chem. C* **2009**, *113*, 17359.
[199] S. A. Díaz, G. O. Menéndez, M. H. Etchehon, L. Giordano, T. M. Jovin, E. A. Jares-Erijman, *ACS Nano* **2011**, *5*, 2795.
[200] P. A. Ledin, M. Russell, J. A. Geldmeier, I. M. Tkachenko, A. M. Mahmoud, V. Shevchenko, M. A. El-Sayed, V. V. Tsukruk, *ACS Appl. Mater. Interfaces* **2015**, *7*, 4902.
[201] K. E. Snell, J.-Y. Mevellec, B. Humbert, F. Lagugne-Labarthet, E. Ishow, *ACS Appl. Mater. Interfaces* **2015**, *7*, 1932.
[202] H. Yamaguchi, K. Matsuda, M. Irie, *J. Phys. Chem. C* **2007**, *111*, 3853.
[203] Y. Shiraishi, K. Tanaka, E. Shirakawa, Y. Sugano, S. Ichikawa, S. Tanaka, T. Hirai, *Angew. Chem. Int. Ed.* **2013**, *52*, 8304.
[204] K. Ouhenia-Ouadahi, R. Yasukuni, P. Yu, G. Laurent, C. Pavageau, J. Grand, J. Guerin, A. Leaustic, N. Felidj, J. Aubard, K. Nakatani, R. Metivier, *Chem. Commun.* **2014**, *50*, 7299.
[205] T. J. Wigglesworth, N. R. Branda, *Chem. Mat.* **2005**, *17*, 5473.
[206] M. Irie, T. Fulcaminato, K. Matsuda, S. Kobatake, *Chem. Rev.* **2014**, *114*, 12174.
[207] J.-K. Sun, P. Wang, Q.-X. Yao, Y.-J. Chen, Z.-H. Li, Y.-F. Zhang, L.-M. Wu, J. Zhang, *J. Mater. Chem.* **2012**, *22*, 12212.
[208] S. M. Sharker, C. J. Jeong, S. M. Kim, J.-E. Lee, J. H. Jeong, I. In, H. Lee, S. Y. Park, *Chem. Asian J.* **2014**, *9*, 2921.
[209] Q. Chen, D. Zhang, G. Zhang, X. Yang, Y. Feng, Q. Fan, D. Zhu, *Adv. Func. Mater.* **2010**, *20*, 3244.
[210] K. Matsubara, M. Watanabe, Y. Takeoka, *Angew. Chem. Int. Ed.* **2007**, *46*, 1688.
[211] N. Crespo-Monteiro, N. Destouches, T. Epicier, L. Balan, F. Vocanson, Y. Lefkir, J.-Y. Michalon, *J. Phys. Chem. C* **2014**, *118*, 24055.
[212] D. K. Diop, L. Simonot, N. Destouches, G. Abadias, F. Pailloux, P. Guerin, D. Babonneau, *Adv. Mater. Interfaces* **2015**, *2*.
[213] T. Nakato, S. Ishida, J.-y. Kaneda, E. Mouri, *J. Ceram. Soc. Jpn.* **2015**, *123*, 809.
[214] F. Tricot, F. Vocanson, D. Chaussy, D. Beneventi, M. Party, N. Destouches, *RSC Adv.* **2015**, *5*, 84560.
[215] L. Bois, F. Chassagneux, Y. Battie, F. Bessueille, L. Mollet, S. Parola, N. Destouches, N. Toulhoat, N. Moncoffre, *Langmuir* **2010**, *26*, 1199.
[216] L. Miao, Y. Ina, S. Tanemura, T. Jiang, M. Tanemura, K. Kaneko, S. Toh, Y. Mori, *Surf. Sci.* **2007**, *601*, 2792.
[217] D. M. Tobaldi, N. Rozman, M. Leoni, M. P. Seabra, A. S. Škapin, R. C. Pullar, J. A. Labrincha, *J. Phys. Chem. C* **2015**, *119*, 23658.
[218] T. He, J. N. Yao, *J. Photochem. Photobiol., C* **2003**, *4*, 125.
[219] T. He, J. Yao, *J. Mater. Chem.* **2007**, *17*, 4547.
[220] H. Ikake, Y. Fukuda, S. Shimizu, K. Kurita, S. Yano, *Kobunshi Ronbunshu* **2002**, *59*, 608.
[221] R. F. de Farias, *Mater. Chem. Phys.* **2005**, *90*, 302.
[222] B. Ingham, S. V. Chong, J. L. Tallon, *J. Phys. Chem. B* **2005**, *109*, 4936.
[223] J. Polleux, N. Pinna, M. Antonietti, M. Niederberger, *J. Am. Chem. Soc.* **2005**, *127*, 15595.
[224] Z. G. Zhao, M. Miyauchi, *Chem. Commun.* **2009**, 2204.

[225] Q. Gao, S. Wang, H. Fang, J. Weng, Y. Zhang, J. Mao, Y. Tang, *J. Mater. Chem.* **2012**, *22*, 4709.
[226] X. X. Liu, L. J. Bian, L. Zhang, L. J. Zhang, *J. Solid State Electrochem.* **2007**, *11*, 1279.
[227] A. I. Gavrilyuk, *Sol. Energy Mater. Sol. Cells* **2010**, *94*, 515.
[228] M. Rouhani, Y. L. Foo, J. Hobley, J. S. Pan, G. S. Subramanian, X. J. Yu, A. Rusydi, S. Gorelik, *Appl. Surf. Sci.* **2013**, *273*, 150.
[229] J. H. Ha, P. Muralidharan, D. K. Kim, *J. Alloy. Compd.* **2009**, *475*, 446.
[230] Y. P. He, Y. P. Zhao, *J. Phys. Chem. C* **2008**, *112*, 61.
[231] W. Chen, H. Shen, X. Zhu, Z. Xing, S. Zhang, *Ceram. Int.* **2015**, *41*, 12638.
[232] T. J. DeJournett, J. B. Spicer, *Solar Energ. Mater. Solar Cells* **2014**, *120*, 102.
[233] Z.-G. Zhao, Z.-F. Liu, M. Miyauchi, *Adv. Func. Mater.* **2010**, *20*, 4162.
[234] A. I. Gavrilyuk, *Sol. Energy Mater. Sol. Cells* **2009**, *93*, 1885.
[235] J. K. Yang, X. T. Zhang, H. Liu, C. H. Wang, S. P. Liu, P. P. Sun, L. L. Wang, Y. C. Liu, *Catal. Today* **2013**, *201*, 195.
[236] J. Zhang, T. He, C. Wang, X. Zhang, Y. Zeng, *Opt. Laser Technol.* **2011**, *43*, 974.
[237] Z. K. Luo, J. J. Yang, H. H. Cai, H. Y. Li, X. Z. Ren, J. H. Liu, X. Liang, *Thin Solid Films* **2008**, *516*, 5541.
[238] S. Yamazaki, H. Ishida, D. Shimizu, K. Adachi, *ACS Appl. Mater. Interfaces* **2015**, *7*, 26326.
[239] A. S. Poulos, D. Constantin, P. Davidson, M. Imperor, B. Pansu, P. Panine, L. Nicole, C. Sanchez, *Langmuir* **2008**, *24*, 6285.
[240] M. Dan-Hardi, C. Serre, T. Frot, L. Rozes, G. Maurin, C. Sanchez, G. Ferey, *J. Am. Chem. Soc.* **2009**, *131*, 10857.
[241] O. Oms, K. Hakouk, R. Dessapt, P. Deniard, S. Jobic, A. Dolbecq, T. Palacin, L. Nadjo, B. Keita, J. Marrot, P. Mialane, *Chem. Commun.* **2012**, *48*, 12103.
[242] K. Hakouk, O. Oms, A. Dolbecq, J. Marrot, A. Saad, P. Mialane, H. El Bekkachi, S. Jobic, P. Deniard, R. Dessapt, *J. Mater. Chem. C* **2014**, *2*, 1628.
[243] A. Parrot, G. Izzet, L.-M. Chamoreau, A. Proust, O. Oms, A. Dolbecq, K. Hakouk, H. El Bekkachi, P. Deniard, R. Dessapt, P. Mialane, *Inorg. Chem.* **2013**, *52*, 11156.
[244] P. Mialane, G. Zhang, I. M. Mbomekalle, P. Yu, J.-D. Compain, A. Dolbecq, J. Marrot, F. Secheresse, B. Keita, L. Nadjo, *Chem. Eur. J.* **2010**, *16*, 5572.
[245] E. P. Ferreira-Neto, S. Ullah, F. L. S. de Carvalho, A. L. de Souza, M. de Oliveira, Jr., J. F. Schneider, Y. P. Mascarenhas, A. M. Jorge, Jr., U. P. Rodrigues-Filho, *Mater. Chem. Phys.* **2015**, *153*, 410.
[246] J. Lu, J.-X. Lin, X.-L. Zhao, R. Cao, *Chem. Commun.* **2012**, *48*, 669.
[247] R. Dessapt, M. Gabard, M. Bujoli-Doeuff, P. Deniard, S. Jobic, *Inorg. Chem.* **2011**, *50*, 8790.
[248] V. Coue, R. Dessapt, M. Bujoli-Doeuff, M. Evain, S. Jobic, *Inorg. Chem.* **2007**, *46*, 2824.
[249] Z.-J. Zhang, S.-C. Xiang, G.-C. Guo, G. Xu, M.-S. Wang, J.-P. Zou, S.-P. Guo, J.-S. Huang, *Angew. Chem. Int. Ed.* **2008**, *47*, 4149.
[250] N. Casan-Pastor, P. Gomez-Romero, *Front. Biosci.* **2004**, *9*, 1759.
[251] P. Horcajada, C. Serre, D. Grosso, C. Boissiere, S. Perruchas, C. Sanchez, G. Ferey, *Adv. Mate.r* **2009**, *21*, 1931.
[252] X. Luo, C. Yang, *Phys. Chem. Chem. Phys.* **2011**, *13*, 7892.
[253] M. de Oliveira, Jr., A. Lopes de Souza, J. Schneider, U. P. Rodrigues-Filho, *Chem. Mater.* **2011**, *23*, 953.
[254] W. Qi, H. Li, L. Wu, *J. Phys. Chem. B* **2008**, *112*, 8257.
[255] Y. Huang, Q. Y. Pan, X. W. Dong, Z. X. Cheng, *Mater. Chem. Phys.* **2006**, *97*, 431.

[256] T. V. Pinto, D. M. Fernandes, C. Pereira, A. Guedes, G. Blanco, J. M. Pintado, M. F. R. Pereira, C. Freire, *Dalton Trans.* **2015**, *44*, 4582.
[257] E. F. Molina, L. Marcal, H. W. P. de Carvalho, E. J. Nassar, K. J. Ciuffi, *Polym. Chem.* **2013**, *4*, 1575.